UPTEC W 21018
Examensarbete 30 hp
Juni 2021

UPPSALA
UNIVERSITET

Analysis of seepage, contaminant transport, compaction and safety of the Zhaoli ditch dam, a tailing reservoir

A modeling study of a tailing reservoir with GeoStudio

Veronika Wei Wang

Analysis of seepage, contaminant transport, compaction and safety of the Zhaoli ditch dam, a tailing reservoir

A modeling study of a tailing reservoir with GeoStudio

Veronika Wei Wang

Abstract

Analysis of seepage, contaminant transport, compaction and safety of the Zhaoli ditch dam, a tailing reservoir

Veronika Wei Wang

In the mining industry, people remove rock from the ground to obtain a metal ore. After processing, the uneconomic fraction called tailings is deposited as a slurry in large reservoirs. The processing adds water and chemical agents to the tailings so that the original structure of the material therefore changes, which make storage of tailings complicated. If a tailing reservoir collapses, it can damage properties and life downstream. In addition, tailings may contain contaminants that disturb living organisms and contaminated groundwater in the local area even under normal operations. Therefore, tracing the contaminants and studying the stability of the tailing reservoirs are important. The aim of the thesis is to investigate seepage, contaminant transport, tailings compaction and slope stability of the Zhaoli ditch tailings reservoir (China) during its construction and afterwards. Simulations are performed with the computer program GeoStudio. According to the simulations and the conditions, contaminant transport was highly related with total head. Total head boundary conditions have also a large effect on slope stability. The area that has most vertical displacement is at the middle of the tailings reservoir, and the greatest change of vertical displacement is located near the slope, where the vertical displacement can increase 0.5 meter over a 10 - 30 meter distance. The slope stability can be different from case to case, but the original designed tailing reservoir have a good safety factor, indicating that the slope is not going to collapse easily.

Keyword: upstream method, Geostudio, tailings reservoir, tailings dam, dam, seepage, contaminant transport, compaction, stability

Department of Earth Sciences, Program for Air, Water and Landscape Science, Uppsala University, Villavägen 16, SE-75236 Uppsala, Sverige.

Referat

Att analysera föroreningstransport, vattenläckage samt stabilitet och säkerhet baserade på Zhaoli ditch dammen

Veronika Wei Wang

Vi människor vill utnyttja malmerna i marken för att skapa ett mer effektivt industrisamhälle. För att utvinna så mycket användbara metaller som möjligt tillsätts kemikalier och vatten under anrikningsprocessen, vilket gör att deponering av de vattenmättade restprodukterna i sandmagasin blir en utmaning med avseende på dammstabilitet och föroreningstransport.

Eftersom det är svårt att ändra på en färdigbyggd damm för anrikningssanden använder detta examensarbete av Geostudio för att simulera hur olika parameter påverka föroreningstransport i dammen, vattenläckage från dammen samt dammens stabilitet och säkerhet. Projektet har simulerat förhållanden i Zhaoli ditch damm i Kina.

Simulering i GeoStudio visar att föroreningsspridning är stark kopplad till den totala hydrauliska potentialen och materialets hydrauliska konduktivitet. Randvillkoren med avseende på den hydrauliska potentialen utanför dammen även har en stor inverkan på dammvallens stabilitet. De största vertikala sättningar sker i mitten av dammen, och den störste sättningsgradient finns i dammvallens sluttning, där en vertikal sättning på 0.5 meter över ett avstånd på 10-30 meter beräknas. Deformation är störst på första lagret över berggrunden. Simuleringarna visar att dammvallens sluttning är stabil med en tillräcklig hög säkerhetsfaktor.

Nyckelord: damm, föroreningstransport, vattenläckage, stabilitet, säkerhet

Institutionen for geovetenskaper, Luft-, vatten- och landskapslära, Uppsala universitet, Villavägen 16, SE-75236 Uppsala, Sverige.

Acknowledgment

This master thesis was carried out at the department of Hydraulic Engineering at Tsinghua University in Beijing, China from February to June 2019.

At first, I would like to thank my supervisor, Professor Liming Hu for the invitation and for providing me with a pleasant working environment. He welcomed me when I had questions, gave me useful advice through interesting discussions, and guided me with good directions.

I would also like to thank all the students who work for Professor Hu. They were always keen on help when I asked, and created a good working environment at the office. They also invited me to different social activities and made the stay more pleasant.

This work was funded by Energiforsk AB within the frame of dam safety, http://www.energiforsk.se. I would like to thank Professor James Yang from Vattenfall R&D and KTH who managed the work and made the trip possible.

Finally, yet importantly, I would like to thank my reviewers, Roger Herbert, Per Norrlund, my tutor, Allan Rodhe, and director of the work program, Fritjof Fagerlund and Rickard Pettersson, at Uppsala University for all their help and suggestions.

Veronika, 2021

Table of Contents

1 Introduction

Tailings are the residues produced during the separation process in hard rock mining, when the valuable fractions are separated from the uneconomic fractions. A common storage option for tailings is to build a tailings reservoir, where the tailings are pumped as a slurry. Tailings reservoirs, however, are structures built of unconsolidated sediments and there is a risk that such reservoirs can collapse. Over the past ten years there have been more than fifty disasters related to tailings reservoirs throughout the world (Bochove et al., 2019). A recent example is a mining dam in Brazil. It collapsed on the 25th of January 2019 causing at least 168 deaths and 141 disappearances (Bochove et al., 2019). Statistics show that the most common reason for tailing reservoir collapse is dam slope instability (Yang et al., 2008). Shear failure is the cause of 34% of all accidents, but other possible causes are overtopping failure, earthquakes, foundation destabilization, foundation compaction, seepage failure and structure failure. This study will simulate a number of processes that can contribute to reservoir collapse.

1.1 Tailings and tailings reservoir construction

In Sweden, 80 percent of the waste is produced by the mining industry. The wastes are formed in several stages of the mining process. Among these, there are three types of waste that stand out due to their large volumes. They are waste rock, tailings and mine water (SGU, 2020). In this study, the focus is only on the tailings.

Tailings are slurries that consist of small particles and fluids from metal ore extraction. After a metal ore is mine, it is finely crushed and mixed with chemicals that allow the separation of valuable metallic minerals from uneconomical gangue minerals. The metal-rich fraction of the slurry is used for metal production, while the remaining material becomes tailings, a waste product. These can contain metals, minerals, chemicals, organics and process water, depending on the property of the ore rocks and the milling process. The particle size can vary from the size of clay to medium sand. Usually tailings contain about 30% solids, but it could be concentrated to 60% solid to help with tailings sedimentation (Blowes et al., 2003).

Tailings can contain both metal-rich minerals and also pore water with dissolved heavy metals and other contaminants. Due to the complex nature of the milling and extraction process, it is hard to name all the contaminants in the tailings, but the pore water in the tailings can contain a highly concentrated metal content that can have a negative impact to the environment (Wong et al., 1977). Therefore, it is important to understand how these dissolved contaminants can be transported from the tailings reservoir into the surrounding environment. This report will track contaminant transport in a tailing reservoir.

When the tailings are separated from valuable minerals, it is pumped as a slurry and sent to a tailings reservoir through a pipe. The reservoir can be constructed in different ways,

depending on the situation. The most common way is to take advantages of the location and the geology near the mining place to reduce the transportation and construction cost. It usually means depositing the tailings on the ground surface in a valley, and building a high soil embankment (dam) in front of it to retain the tailings. Therefore, water and particles can discharge from the dam or through the ground, if the permeability is not too low (SGU, 2020).

There are many methods to store tailings and the upstream method is one of them. The construction of the upstream method starts with building an initial dam at the opening of a valley. Through a pipe, tailings are poured behind the dam wall into the reservoir. Particles with large diameters deposit faster and therefore travel shorter distances than smaller particles. The construction method takes advantage of this phenomenon by placing the pipe near the top of the initial dam. As the bigger particles settle down near the dam wall and dry out, they became part of the slope. The pipe is moved along the slope to higher places to make the slope grow as tailings are poured into the system (Vick, 1983). Other methods that differ from the upstream method are to reinforce the slope in different forms (e.g. downstream method) or remove some of the water in tailings before the tailings are sent to the reservoir as so-called thickened tailings (Vick, 1983).

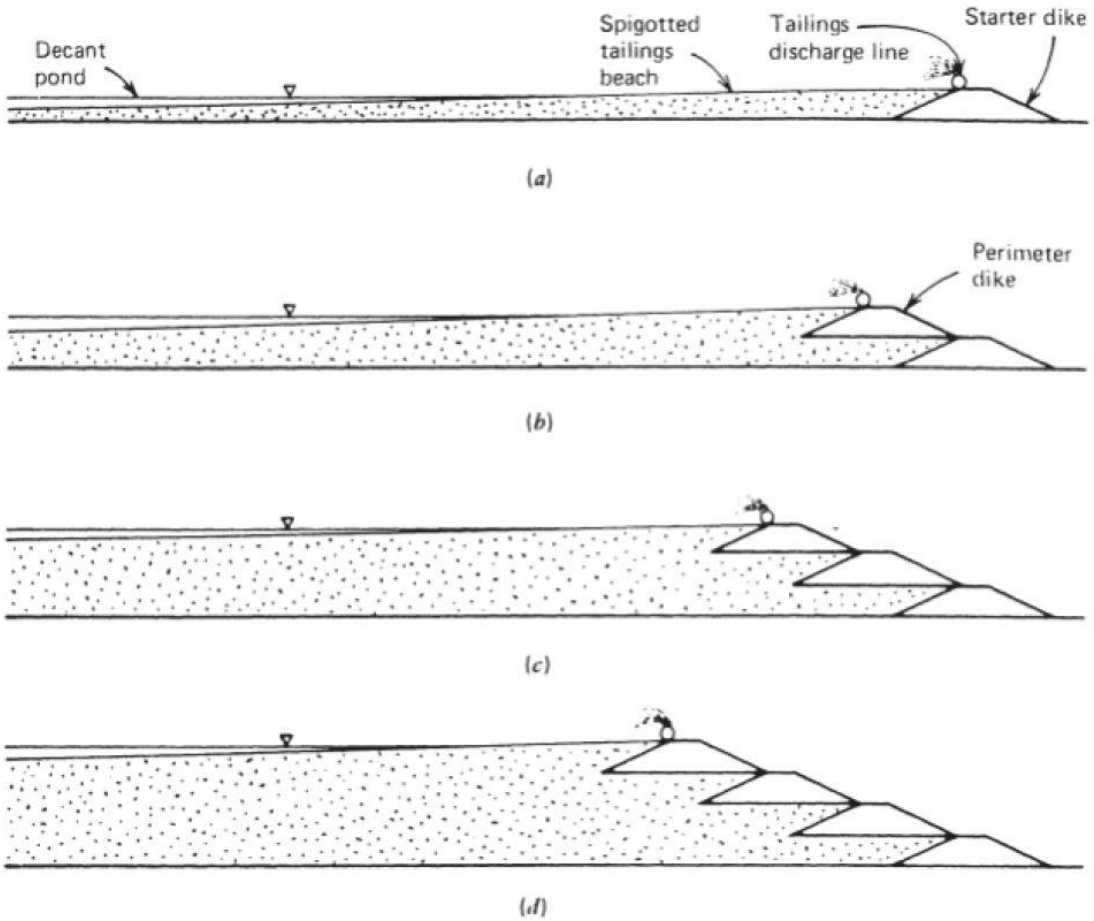

Figure 1. A tailing reservoir built by upstream method (Vick, 1983).

The upstream method is widely applied in the industry due to its easy construction, low initial cost, and low maintenance cost. Unfortunately some people assume that a low maintenance cost is the same as a stable structure. However, slope stability is a concern with the upstream method and stability can change under different conditions. For example, if the tailings are discharged with a high flowrate and high water content, the water can seep into the dam walls and lead to a pore pressure increase; such pore pressure increases might lead to slope collapse (Davies, 2000). In other words, any reason that makes the water content increase has the potential to damage the slope. In this report, slope stability is investigated by simulating different total heads and construction processes. In addition, the construction process is simulated by considering the layer-by-layer effect of tailings weight on other layers, which might cause deformation and negatively impact the stability of the slope.

1.2 Aim and question formulation

The aim of the thesis is to simulate seepage, contaminant transport, tailings compaction and slope stability of the Zhaoli ditch tailings reservoir (China) during its construction and afterwards. Simulations are performed with the computer program GeoStudio.

Based on a number of concerns with regard to contaminant transport and dam safety, the thesis attempts to answer the following questions:

- What does the contaminant transport in the tailing reservoir look like when construction is completed?
- Which part of the tailings reservoir has the biggest displacement?
- What factors influence the stability of the tailings reservoir, and which part of the tailings reservoir is most unstable?

1.3 Delimitations

Due to the high-efficiency calculations from GeoStudio, it is easier to simulate a tailings reservoir compared to constructing a real dam. Therefore, it is important to understand the relations between parameters and real situations. Data used under simulation were selected carefully according to previous research and interviews of people with experience. Readers should still be aware that results are only applicable to the simulations in the report, under the conditions described in the method section.

Calculations by the program do not include climate and vegetation contributions, and there is no water evaporation from the ground. Soil mechanics is complicated and there are geotechnical issues that cannot be easily described with the equations. Because of the

complex nature of the simulations, the equations used in the program have been simplified (Geoslope, 2012b).

2 Theory

The theory in the following section relates to the processes simulated in this project, namely seepage, contaminant transport, compaction and stability.

Simulations in this work are presented in one or two dimensions, but the real problems are in three-dimensional space. It means three dimensional equations are needed to give a better understanding about the situations. In this section, equations are presented in one, two and even three dimensions.

Nomenclature can be found in the Appendix.

2.1 Seepage

In this section, theories on soil hydraulic conductivity, Darcy's law and seepage velocity are presented.

2.1.1 Liquid transport inside a soil

In order to understand fluid migration inside soil it is helpful to start with the energy balance. When fluid velocity increases, the pressure or potential energy of the fluid will decrease for isotropic flows. Isotropic flows are flows with no energy transformation, in which no extra heat enters or leaves from the system. It means that the sum of the kinetic, potential and internal energy in a fluid is equal on all points along a streamline, this is known as conservation of energy (Clancy, 1975). Therefore, if the flow is incompressible, the total head of the flow can be written in the form,

$$H = z + \frac{u}{\gamma_w} + \frac{v^2}{2g} \ , \tag{2.1}$$

where z presents a term for potential energy, the energy from the elevation. The pressure head, $\frac{u}{\gamma_w}$, representing a term for internal energy. The dynamic pressure is $\frac{v^2}{2g}$, which is the kinetic energy of a flowing fluid per unit volume. The total head, H is the sum of all terms. The hydraulic head, *h*, is the sum of *z* and $\frac{u}{\gamma_w}$, and it is widely used due to the dynamic pressure term is negligible.

The hydraulic head is different at different locations in the soil. Water in soil pores will flow from the higher hydraulic head to the lower. Energy loss under transport between two points is called head loss ΔH. Hydraulic gradient, i describe relation between the head loss and the

distance, *L* (Li et al., 2013). The relation can be simplified as

$$i = \frac{\Delta H}{L}. \tag{2.2}$$

2.1.2 Darcy's law and seepage

Different hydraulic head at two locations makes water move in the soil, this is known as seepage. It exists as long as the water content and the total head difference inside the soil is not zero. Darcy's velocity q_w describes the relationship between the hydraulic gradient and hydraulic conductivity as

$$\begin{bmatrix} q_{wx} \\ q_{wz} \end{bmatrix} = -\begin{bmatrix} k_x & k_{xz} \\ k_{zx} & k_z \end{bmatrix}\begin{bmatrix} i_x \\ i_z \end{bmatrix} \quad . \tag{2.3}$$

The hydraulic conductivity conductivity, k, describes how well a soil can transport water. For example, in an isotropic soil, the seepage velocity and hydraulic gradient are aligned, which means k_{xz}=k_{zx}=0 and k_x=k_z. Anisotropic soil has different characteristics in different directions, therefore k_x, k_{xz}, k_z and k_{zx} become different.

Fluid entering a small soil element selected randomly from the soil can be described with

$$\mathrm{dq}_e = \mathrm{v}_x dz \cdot dy + \mathrm{v}_z dx \cdot dy, \tag{2.4}$$

and fluid leaving the element can be described with

$$\mathrm{dq}_o = (\mathrm{v}_x + \frac{\partial \mathrm{v}_x}{\partial x} dx) dz \cdot dy + (\mathrm{v}_z + \frac{\partial \mathrm{v}_z}{\partial z} dz) dx \cdot dy. \tag{2.5}$$

Combining the assumption that the fluid inside the soil element is incompressible and the principle of continuity, the water flow entering and leaving the soil volume are equal to each other

$$\mathrm{dq}_\mathrm{e} = \mathrm{dq}_o \tag{2.6}$$

which gives that

$$\frac{\partial \mathrm{v}_x}{\partial x} + \frac{\partial \mathrm{v}_z}{\partial z} = 0 \ . \tag{2.7}$$

Combining equation (2.7) and Darcy's law will result in the following equation

$$\frac{\partial^2 h}{\partial x^2} + \frac{\partial^2 h}{\partial z^2} = 0 \ . \tag{2.8}$$

Equation (2.8) is called the Laplace equation. The assumptions made in this equation are that hydraulic conductivity k is unchanging, water always flows in and out of the soil volume without stopping, and the porous medium is isotropic and homogeneous (Verruijt, 2001).

$$\frac{\partial}{\partial x}\left(k_x \frac{\partial H}{\partial x}\right) + \frac{\partial}{\partial z}\left(k_z \frac{\partial H}{\partial z}\right) + Q = \frac{\partial \theta}{\partial t} \tag{2.9}$$

Equation 2.9 is a differential equation and applies to two- dimensional tailing seepage problems (Li et al., 2013). Volumetric water content changes over time as $\frac{\partial \theta}{\partial t}$, which indicates that the soil volume can be completely water saturated, or only partially water-saturated. Hydraulic conductivity in (x, z) direction is k_x and k_z. Source flow is Q.

2.1.3 Water transfer in GeoStudio with Seep/W

'Soil' can be simplified as a mixture of air, water and soil skeleton. Since its mass contains three elements, the changing of mass can depend on changing water content. In GeoStudio, Seep/W is used to calculate fluid transfer and storage in soil pores. The calculations are based on the theory of Domenico and Schwartz (1998). The mass change in the stored mass over time $\dot{M}_{st}$, equals the difference between in- and outflow and the change in mass inside the soil skeleton, $\dot{M}_S$

$$\dot{M}_{st} = \frac{dM_{st}}{dt} = \dot{m}_{st} - \dot{m}_{out} + \dot{M}_S, \tag{2.10}$$

and $\dot{M}_{st}$ can be divided into liquid $\dot{M}_w$ and water vapor $\dot{M}_v$, then

$$\dot{M}_{st} = \dot{M}_w + \dot{M}_v\ . \tag{2.11}$$

By using Darcy's law it is able to calculate the mass flow rate of liquid water and Fick's law to calculate the mass flow rate of water vapor. An equation for $\dot{M}_w$ can be

$$\dot{M}_w = \rho_w \left(\theta_w \beta_w \frac{\partial u_w}{\partial t} + \beta \frac{\partial u_w}{\partial t} + m_w \frac{\partial \varphi}{\partial t}\right) + \theta_w \rho_w \alpha_w \frac{\partial T}{\partial t}\ . \tag{2.12}$$

Equation (2.12) is used to calculate the liquid water transfer and the storage in a soil element due to pore-water pressure. This form is used to define material in Seep/W. Fluid in the form of vapor, $\dot{M}_v$ is calculated by GeoStudio using

$$\dot{M}_v = \frac{M}{R}\frac{\partial}{\partial t}\frac{(p_v V_a)}{T} = \frac{M}{R}\frac{\partial}{\partial t}\frac{(p_v \theta_a)}{T} dx\ dy\ dz. \tag{2.13}$$

In some cases, it is needed to calculate how the mass flow rate changes. It has contributions from both liquid and vapor water. The water motion is driven by the energy gradient

$$\dot{m}_w = \rho_w q_w dxdz = \frac{-K_w}{g}\left(\frac{\partial u_w}{\partial y} + \rho_w g \frac{\partial y}{\partial y}\right) dxdz. \quad (2.14)$$

Equation 2.15 is a hydraulic conductivity function. It calculates how diffusion affects the mass flow rate.

$$\dot{m}_v = -D_v \frac{\partial p_v}{\partial y} dxdz,\ D_v = \tau\theta_a D_{vap} \frac{M}{RT} \quad (2.15)$$

When tailings desiccate, the surface becomes unsaturated and matric suction changes, this is simulated in the model. Matric suction is related to volumetric water content and hydraulic conductivity, when material is defined. If a model is used as 'saturated only', this assumes that water content is unchanged as time goes by (Geoslope, 2018).

2.2 Contaminant transport

In this section, theory relating to bulk motion of contaminants, and calculations in GeoStudio are presented.

2.2.1 Diffusion, advection and dispersion of contaminants

Contaminants bulk motion can be divided into three parts: diffusion, advection and mechanical dispersion. Diffusion refers to the fact that contaminants flow from higher chemical potential (concentration) to lower. Advection describes how contaminants are transported with a fluid. The velocity of a fluid can be seen as a vector field, and contaminants concentration as a scalar field. Mechanical dispersion is used to describe the contribution from twisted paths created by the soil skeleton and pores. For examples, bigger pores will be easier to pass than smaller ones, because of friction, and fluids that have the same velocity but different trajectories spread differently (Bear, 1972). In general, diffusion has less effect on contaminant transport than dispersion due to the generally low concentration of contaminants. Thus, physical obstacles from the soil skeleton have a greater impact on contaminant transport.

2.2.2 Hydrodynamic dispersion

Hydrodynamic dispersion, D, can be described as a combination of mechanical dispersion, D', and diffusion, D^*, then

$$D = D' + D^*. \tag{2.16}$$

Mechanical dispersion is related with seepage velocity, u_d:

$$D'_L = \alpha_L \cdot |u_d|$$
$$D'_T = \alpha_T \cdot |u_d|. \tag{2.17}$$

The longitudinal coefficient is D'_L and transverse mechanical dispersion coefficient is D'_T. The dispersivity coefficient is α. Longitudinal dispersivity varies between 0.001 and 5 m for different types of soils according to data from laboratory. The more similar in size the particles are, the smaller is the number. The most common values lie between 0.1 and 1.0 m. For transverse dispersivity, α_T, values vary between 0.1 and 0.3 of α_L.

(Wang, 2008)

2.2.3 Contaminant transfer in GeoStudio, Ctran/W

In Ctran/W, the changing of stored mass can include contributions from contaminants. The additional part of $\dot{M}_{st}$ can be divided it into dissolved $\dot{M}_{dp}$ and adsorbed phases $\dot{M}_{ap}$

$$\dot{M}_{st} = \dot{M}_{dp} + \dot{M}_{ap} \tag{2.18}$$

The equation (2.19) contains concentration changes with time on the left side. On the right side, diffusion, adsorption, and advection-dispersion in the y-direction are considered

$$\left(\theta_w + \rho_d \frac{\partial S^*}{\partial C}\right)\frac{\partial C}{\partial t} + C\frac{\partial \theta_w}{\partial t} = \frac{\partial}{\partial y}\left[D\theta_w \frac{\partial C}{\partial y} - C q_w\right] - \lambda(\theta_w C + \rho_d S). \tag{2.19}$$

(Geoslope, 2018).

2.3 Stress and compaction

During construction, the tailings reservoir increases in size and weight, and the downward pressure increases accordingly. The increasing pressure can create a vertical deformation on soil called compaction. Deformation of soil is not directly related to the total force acting on the soil, since the soil is a mixture of water, air and the soil skeleton. Different materials behave differently. In 1923, Terzaghi came up the principle of effective stress and consolidation theory to solve this problem for saturated soil (Li et al., 2013).

Most of the mathematical expressions that are presented in this section are used by GeoStudio. The program simulates the consequences of tailings compaction.

2.3.1 Material strength

When a force works on a material, it can seem as a deforming force per area, called stress. At the same time the material can be deformed during the work, meaning the shape or distance between two points in the material can be changed. The strain is the ratio of changing distances before and after the work, and it is unitless. The relation between stress and strain can be linear until a yield point. Before the yield point, the material is elastic, and afterwards it is plastic. The yield criterion used in this thesis is called the Mohr-Coulomb yield criterion.

How shear stress τ acts on the material depends on cohesion c, the normal stress on the shear surfaces between the two materials σ_n, and the angle of internal friction ϕ,

$$\tau = c + \sigma_n tan\phi. \tag{2.20}$$

Mohr's circle rewrites the state of stress on the soil element to a circle in the σ_n- τ plane (Figure 2). Equation (2.20) gives a line in the σ_n- τ plane, which represents the limit-equilibrium state of a soil material. If the line crosses the Mohr's cycle it means that the soil becomes unstable and so-called shear failure occurs (Geoslope, 2015).

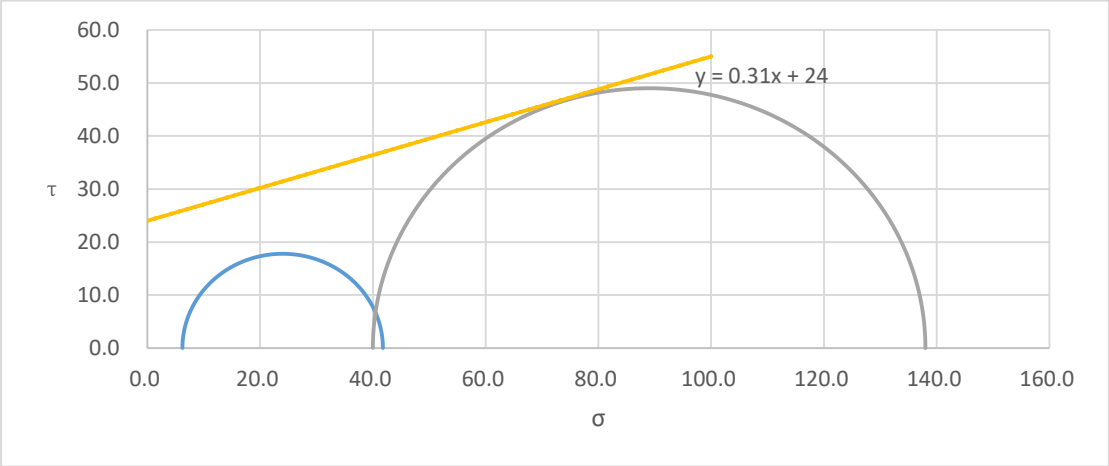

Figure 2. Mohrs circle. The line can be calculated by equation (2.20).

2.3.2 Effective stress σ'

When a force acts on saturated soil, it will only act on the soil skeleton and water. Force that

acts on the soil skeleton transfers as ‘interparticle force’. The force that acts on the water in the pores transfers as ‘pore water pressure’.

In order to build an equation that describes how stress acts on soil, one starts by choosing a cross-section of a saturated soil. Vertical forces on the cross section are referred to as P_{svi}. The sum of the horizontal forces are zero, otherwise the soil will move to right or left. Pore water pressure is u. The vertical stress is σ. Then the force on the cross section can be written as

$$\sigma A = \sum_{i=1}^{n} P_{svi} + uA_w \;\leftrightarrow\; \sigma = \frac{\sum_{i=1}^{n} P_{svi}}{A} + \frac{uA_w}{A}, \tag{2.21}$$

where $\sum_{i=1}^{n} P_{svi}/A$ describes total vertical stress acting on the soil skeleton, which is known as effective stress σ'. The total area of all touchpoints along the cross section, A_s, is in general, 3% of A, and the rest of the place will be full of water. Therefore, A_w is almost equal to A, and A_w/A becomes almost one. The total stress for saturated soil is usually written as

$$\sigma = \sigma' + u. \tag{2.22}$$

(Li et al., 2013)

2.3.3 Compaction

A common type of location chosen for dam construction is where the bedrock is made of highly over-consolidated materials. The main advantage of such selection is that it avoids many problems, such as that the bedrock will not compact significantly, and compaction of tailings becomes the only problem left. To avoid compaction from increasing suddenly, tailings are poured into the reservoir with low speed, but the compaction still exists.

Different materials compact differently, due to their different stress and strain tolerances. In the thesis, linear elasticity was used to simulate the material compaction. The relation between elastic modulus, E and stress σ can use the following equation

$$\begin{Bmatrix} \sigma_x \\ \sigma_y \\ \sigma_z \\ \tau_{xy} \end{Bmatrix} = \frac{E}{(1+v)(1-2v)} \begin{bmatrix} 1-v & v & v & 0 \\ v & 1-v & v & 0 \\ v & v & 1-v & 0 \\ 0 & 0 & 0 & \frac{1-2v}{2} \end{bmatrix} \begin{Bmatrix} \varepsilon_x \\ \varepsilon_y \\ \varepsilon_z \\ \gamma_{xy} \end{Bmatrix}, \tag{2.23}$$

Where Poisson’s ratio, v describes the ratio of deformation. When Poisson’s ratio is 0.5, the volume does not change. However, if the ratio is smaller than 0.5, then the volume is smaller than the initial status.

The stiffness of the soil can be described by the elastic modulus, E- modulus, here $E=\Delta\sigma/\Delta\varepsilon$,

and it can be rewritten with a and e,

$$\mathrm{E} = \frac{\Delta p}{\Delta \varepsilon_z},\ \Delta \varepsilon_z = \frac{\Delta e}{1+e_0},\quad a = -\frac{\Delta e}{\Delta p} \tag{2.24}$$

where e is the porosity and a is the coefficient of compressibility. For a soil with low compressibility, a is usually smaller than 0.1.

In the case that the E- modulus cannot be measured, the Oedometric modulus, E_s can be measured instead. Therefore in the Method section, *E* would be calculated by E_s.The relation between them can describe with

$$E = E_s \cdot \left(1 - \frac{2\upsilon^2}{1-\upsilon}\right). \tag{2.25}$$

(Li et al., 2013)

2.4 Slope stability

In this section, theories relating to slope stability are presented. As mentioned in the introduction, the dam slope can be the weakest part in a tailing reservoir. Shear failure means the slope of the tailing reservoir is unstable and in reality it is manifested as dam collapse. Therefore it is important to study slope stability.

2.4.1 Safety factor

Shear strength of soil includes two parts: rubbing and cohesive strength. They exist more or less between every small soil element in the soil. Cohesion strength unites particles in the soil and makes them unable to slide from the slope, but when shear failure happens, the cohesion strength leads to the entire slope failing. Soil moves along a slip surface (see figure 3). In 1915, K. E. Petterson simplified the problem assuming that when a slip surface slides from the soil, it seems like part of a circle rotates around center of the circle (Li et al., 2013).

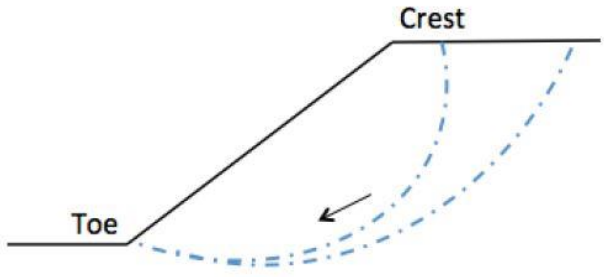

Figure 3. Two potential slip surfaces (Graig, 2004).

In a rotation problem, it is possible to calculate the moments. There are two moments in the system, the moment that makes the soil rotate, M_s and the friction against the movement, M_{R2}. The ratio between these, F_s, can be used as a safety factor

$$F_s = \frac{M_{R2}}{M_s}. \quad (2.26)$$

A lower F_s means that the slip surface is more unstable. It is an index to measure in which part of the dam shear failure is the most likely to occur. It only takes one shear failure to destruct a tailing reservoir; therefore, more attention needs to be paid to the slip surface with the lowest safety factor. When F_s become lower than 1, it usually means shear failure occurred.

The finite stress method was used to calculate the safety factor. It regards the soil element as a deformation body instead of a rigid body. It divides the soil into many elements and calculates the stress and strain, nodal force and displacement on every node. Then it sums up all shear strengths and the frictions along every potential slip surface (Geoslope, 2015).

3 Method

In this section, field site is first presented, and then the model GeoStudio is described. Then, the simulations to be performed in this study are described, and methods of selecting data for parameters and boundary conditions are shown.

3.1 Site description

The field site for this study, the Zhaoli ditch tailings reservoir, is located in China (see Figure 4). It was planned to hold residues from an iron mine, which was 97% siderite (iron carbonate). More detail information about tailings composition is presented in section 3.3.

Figure 4. Location of the Zhaoli ditch tailings reservoir marked with red. Source: Google Maps

For this project, the design of the Zhaoli ditch tailing reservoir was received from Tsinghua University. In 2016, a group of students did a master thesis about the tailing reservoir focusing on the safety of the dam with two different elevations (Bäckström & Ljungblad, 2016).

For modelling, the Zhaoli ditch tailing reservoir can be divided into several sections. The bottom layer is called bedrock in the model, and it is covered by a one-meter thick drainage layer that made of course- grained material, here named the “cover”. It is composed of material that is similar to that of the initial dam and offers a water flow path to reduce collapse risk. The initial dam is 60 m high. It keeps incoming tailings inside a valley that now has become a tailings reservoir.

The dam was filled with a tailings slurry. During deposition (cf. Figure 1), courser materials sedimented closest to the tailings discharge line, and finer materials further away. The modeled cross-section of the Zhaoli ditch tailings reservoir is shown in Figure 5. Next to the initial dam lies the coarse-grained material (called 'coarse' in Figure 5), which has the largest particle size. Further from the discharge line lies finer-grained material, with ‘fine’ material having a larger grain-size than ‘slurry’ material. The section that is furthest away from the initial dam is named ‘slurry’, which contains most fluid and the smallest particles.

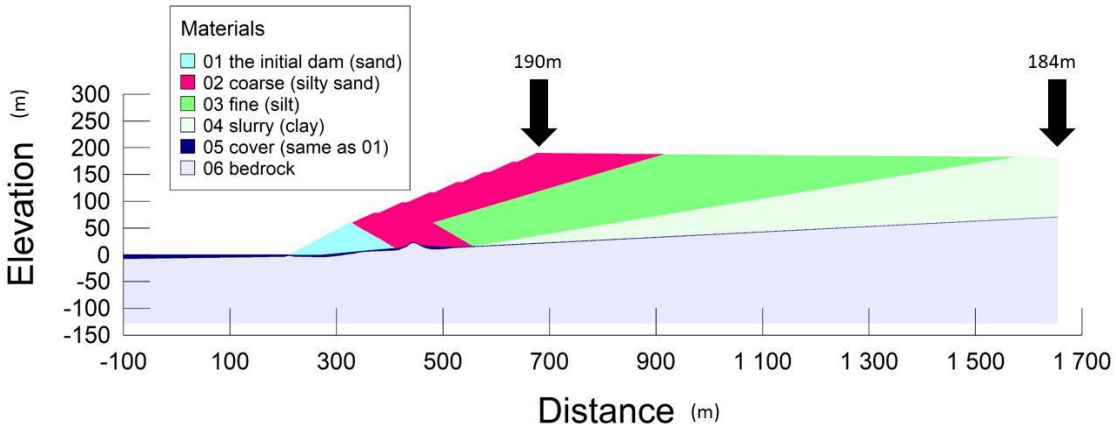

Figure 5. Image of the tailing reservoir constructed in GeoStudio. The surface elevation of the tailing reservoir is not completely horizontal and varies from 184m to 190m.

There is a ditch that lies three meter beyond the initial dam with a depth 1 meter. In this work, the conditions of the ditch never change. Therefore, contributions from the ditch can be ignored.

3.2 GeoStudio

GeoStudio 2018 R2 was made for simulating geotechnical problems, and contains many modules. Seep/W, Ctran/W, Sigma/W and Slope/W were used in this project. Seep/W is specialized on the movement of groundwater between soil grains. The soil can be saturated or unsaturated (Geoslope, 2012b). Ctran/W is specialized on solute and contaminant transport in soil structures (Geoslope, 2012a). Sigma/ W is specialized on simulating simple linear elastic deformation (Geoslope, 2013). Slope/W is used to calculate the stability of a slope (Geoslope, 2015). These programs use the finite element method (FEM) to solve problems. The mechanics behind a tailing reservoir are complicated, and it contains space- and time-dependent problems. Generally, we describe those problems with partial differential equations (PDE), but they cannot be solved with analytic methods. Fortunately, by using different types of discretization, the FEM can rewrite PDEs to numerical model equations and finds numerical solutions (Comsol, 2017).

Finite element size was set to 5 m in ‘Draw Mesh Properties’, as this was considered to be an appropriate size to divide materials into and to enable presentation of results with continuing lines instead of choppy lines.

To construct a 2D tailings reservoir in GeoStudio, the first step was to draw points, lines and regions according to the physical design of the reservoir and then divide the tailings reservoir into sections and define the properties of the material in every section. As shown in Figure 5, there are six types of materials in the description of the reservoir: coarse sediments, dam material, fine sediments, drainage material (“cover” in Figure 5), bedrock and slurry.

3.3 A model in the GeoStudio

To build a tailing reservoir in the GeoStudio, parameters needed to be defined such as hydraulic conductivity, diffusion, dispersivity, stress, and the E- modulus. In this section data that used to build a model in GeoStudio is presented.

Samples of ‘fine’ and ‘coarse’ sediments from the Zhaoli ditch mine were collected in a different study but were used in this study. They were sent to the laboratory at Tsinghua University for analysis. Therefore, data about ‘fine’ and ‘coarse’ sediments were acquired from actual samples, while data on other sediments (e.g. dam wall materials, tailings slurry) were defined by a combination of literature review and experience.

3.3.1 GeoStudio Seep/W

To suit the aims of the study, all materials were set to model ‘saturated or unsaturated’ conditions, instead of always ‘saturated’. The key parameters here are hydraulic conductivity and volumetric water content (VWC). Hydraulic conductivity is related to the change of matric suction, and it is calculated automatically by GeoStudio, when saturated hydraulic conductivity is given. The saturated hydraulic conductivity is shown in the table 3.1 for the materials. The values were determined by combination of data from laboratory and discussions with Professor Hu and his students.

Table 1 Saturated hydraulic conductivity for the tailing reservoir.

	Saturated hydraulic conductivity, *k* (m/s)
Dam	$1 \cdot 10^{-5}$
Coarse	$1.98 \cdot 10^{-7}$
Fine	$1.76 \cdot 10^{-7}$
Slurry	$5 \cdot 10^{-8}$
Cover	$1 \cdot 10^{-5}$
Bedrock	$1 \cdot 10^{-8}$

To fulfill the purpose of the thesis, water seepage had to be calculated for two situations. One situation corresponded to the moment when the tailing reservoir reached its full capacity (see Figure 6) and one to the moment when the tailing reservoir had reached an age of 100 years (see figure 7).

In the first case, due to the tailing reservoir was recently built, total head at upper right corner is determined by the surface elevation (see Figure 5), therefore set the boundary condition total head to 184m. Boundary condition at lower left corner represents ground water or a stream, therefore it is assumed unchanged in both cases. The total head is set to -20m. So do the ditch that lay behind the initial dam had a total head of always -1 meter, due to the depth is 1m below the ground surface, which was assigned an elevation of 0.

In the second case, it is a calculation based on the first case to simulate how groundwater table changes after 100 years. Therefore the boundary condition at the upper right corner was removed since the tailings were no longer water saturated. The boundary conditions for this situation are shown in Figure 7.

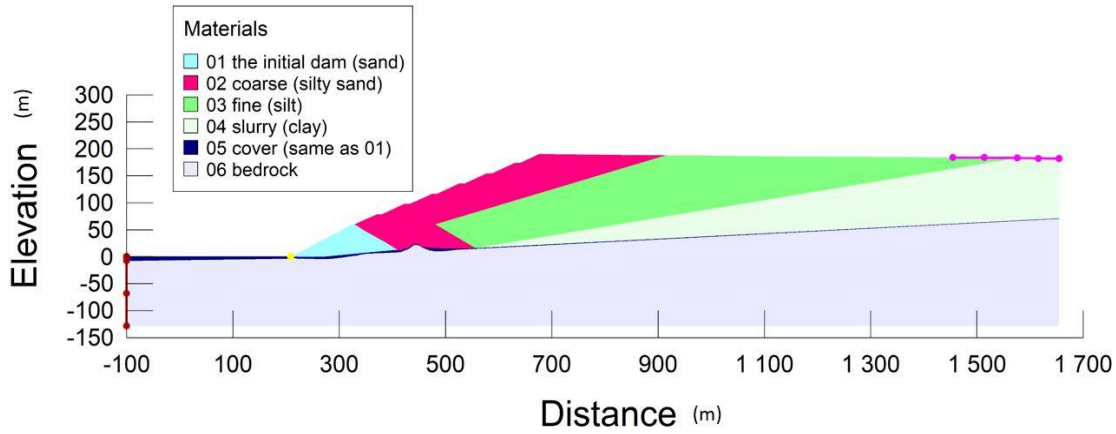

Figure 6. Boundary conditions for the first seepage calculation, at steady state. The purple line at the upper right corner shows a specified total head of 184m. The dark red line at the left corner total head represents a specified total head of -20m. The yellow dot represents where the ditch is located and total head is -1m.

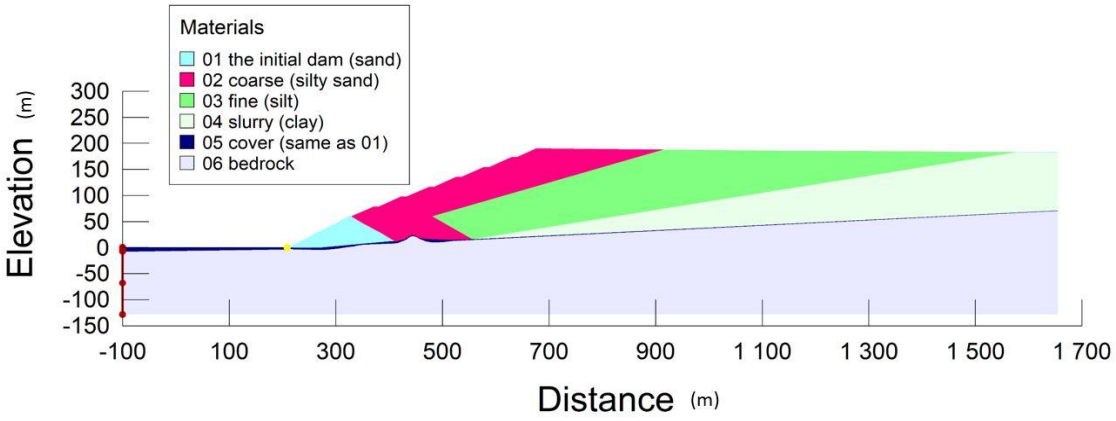

Figure 7. Boundary condition for second seepage calculation, transient, 36500 days (100 years). The boundary condition (dark red line) at the left corner still has a total head of -20m.

3.3.2 GeoStudio Ctran/W

The initial contaminant concentration in the tailings (‘coarse’, ‘fine’ and ‘slurry’ materials) was set to 10 g/m^3, and was assumed to be a non-reactive solute such as chloride. There was no initial contaminant in the materials dam, cover and bedrock. Water flow for these

simulations was based on Seep/W and the same boundary conditions were used as in that section.

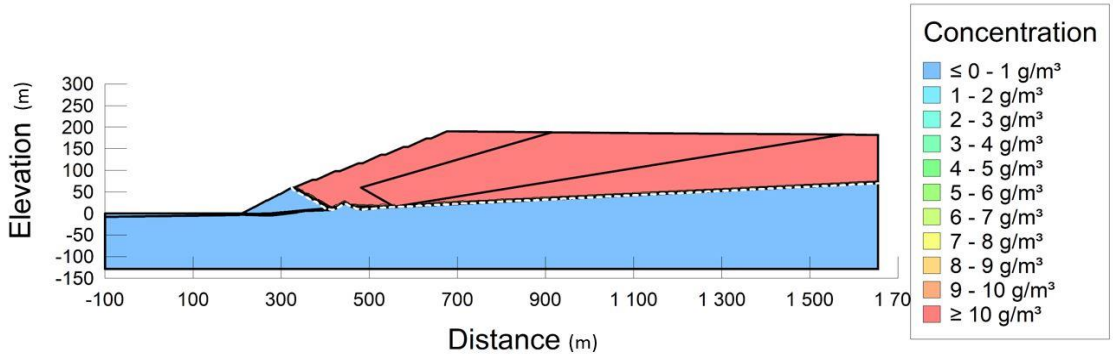

Figure 8. Initial conditions for contaminant concentration distribution. The white dashed line shows the edge of the tailings.

Diffusion of contaminants was referenced to chloride diffusion in different tailing reservoirs. The calculations do not consider adsorption. Diffusion of chloride ions can vary between $1.5 \cdot 10^{-12}$ m^2/s and $4.25 \cdot 10^{-12}$ m^2/s in different kinds of tailings (Song et al., 2017).

Due to particles in the tailing reservoir consolidating by gravity, pore sizes change gradually in horizontal direction, and pore size in the same sections become similar. Dispersivity therefore varied in a small range, numbers between 0.1- 1m were chosen according to theory section 2.2.2. Previous experience has shown that dispersivity in reality may be 100 to 1000 times larger than in laboratory tests (Hu, 2019). The numbers in Table 2 were therefore much bigger than 1m. The transverse dispersivity coefficient, α_T, is twenty percent of longitudinal dispersivity according to theory. The final numbers are shown in table 3.2.

Table 2. Diffusion coefficient and dispersivity used in the tailing reservoir model. The assignment of the longitudinal dispersivity values was somewhat arbitrary, but it was assumed that the bedrock had the highest value, and the slurry had the lowest value.

	Diffusion, D^* (m^2/s)	Longitudinal Dispersivity (m)	Transverse Dispersivity (m)
Dam	$3 \cdot 10^{-12}$	10	2
Coarse	$2.5 \cdot 10^{-12}$	8	1.6
Fine	$3 \cdot 10^{-12}$	6	1.2
Slurry	$4 \cdot 10^{-12}$	5	1
Cover	$3 \cdot 10^{-12}$	10	2
Bedrock	$1.5 \cdot 10^{-12}$	20	4

The calculations for contaminant transport were started from the day the tailing reservoir was just fully filled to 100 years after, both case in method 3.3.1 GeoStudio Seep/W was used to calculate contaminant transport.

To look into more detailed contaminant transport, ten particles were studied using particle

tracking in GeoStudio. Selected particles were on a horizontal or vertical line to investigate the difference in particle migration at different depths and elevations and in different materials. Particle 6 lies on the intersection.

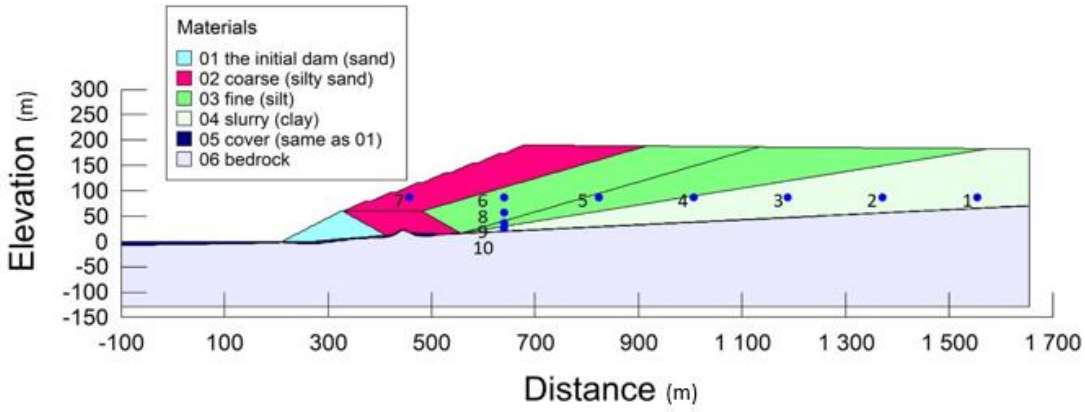

Figure 9. Initial position of ten particles released for particle tracking.

Table 3. Coordinates of the ten particles for particle transport modelling.

Solute particles	Horizontal coordinate (m)	Vertical coordinate (m)
1	1554	87
2	1372	87
3	1189	87
4	1006	87
5	823	87
6	640	87
7	457	87
8	640	57
9	640	36
10	640	26

3.3.3 GeoStudio Sigma/W

For the compaction simulations, the tailing reservoir was divided into 8 layers in order to see the compaction in each layer. It is assumed that every layer takes 100 days to fill or construct (exact times are unknown). Effective E-modulus, unit weight and Poisson's ratio were defined for every layer. The material model used in the section was a 'linear elastic model'.

Oedometric modulus, E_s, of the soil samples was measured in the laboratory in a different study. It varies when stress changes. According to experiences the max and min total stresses are around 900 and 2000 kPa, respectively, and E_s for stress between 800-1600 kPa was therefore chosen. Then equation (2.25) was used to calculate E- modulus:

Table 4. Oedometric modulus (E_s). The orange color is the data which has been selected. Data from laboratory experiments conducted in different study.

Stress (kPa)	100-200	200-400	400-800	800-1600	1600-2000
Fine	6.08	10.24	17.32	28.43	39.18
Coarse	5.42	9.09	15.52	25.5	36.49

Table 5. Selected parameters for simulating materials with the linear elastic method. Parameters for Coarse and Fine were measured. Parameters estimated for Dam, Slurry, Cover and Bedrock.

	E- modulus, E (kPa)	Unit weight (kN/m^3)	Poisson's ratio, ν (−)
Dam	25000	21.2	0.3
Coarse	21250	21.4	0.25
Fine	17714	21.5	0.35
Slurry	15000	20	0.4
Cover	25000	20	0.2
Bedrock	300000	26	0.18

The horizontal displacements on the right edge were set to zero. For the left edge and baseline, the horizontal and vertical displacements were set to zero. Those are the boundary conditions in this section.

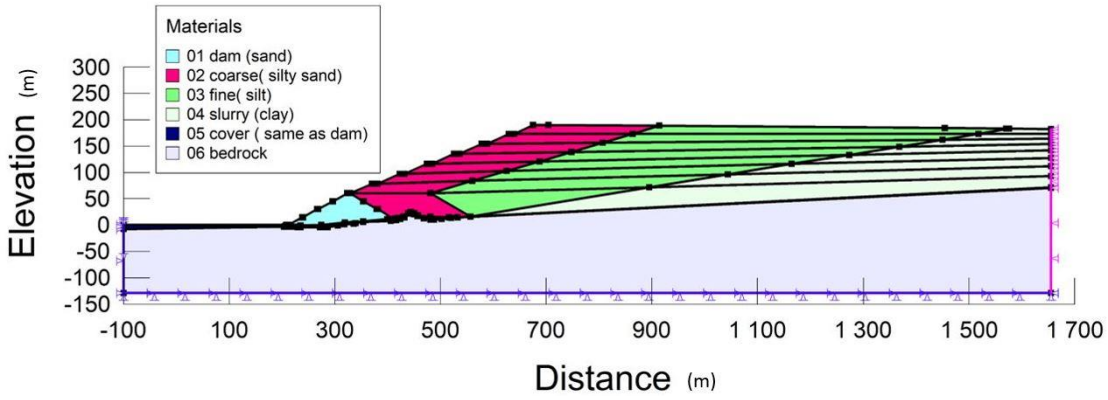

Figure 10. Boundary conditions for deformation marked with blue and purple lines. The black lines represent separated layers where each layer takes 100 days to fill.

3.3.4 GeoStudio Slope/W

The stability tests were based on calculations from 'Sigma/W'. Material properties were defined as shown in table 6.

Table 6. Material properties of Slope/W. Parameters for Coarse and Fine were measured. Parameters for Dam, Slurry, Cover and Bedrock were estimated.

	Dam	Coarse	Fine	Slurry	Cover	Bedrock
Unit weight (kN/m^3)	21.2	21.4	21.5	20	20	26

Cohesion, *c* (kPa)	0	0	0	0	0	1000
Phi, ϕ (degree)	40	41.5	38.1	15	38	50

The slip surface entry and exit range were drawn to help the program calculate the unsafe locations. (Shown in Figure 11)

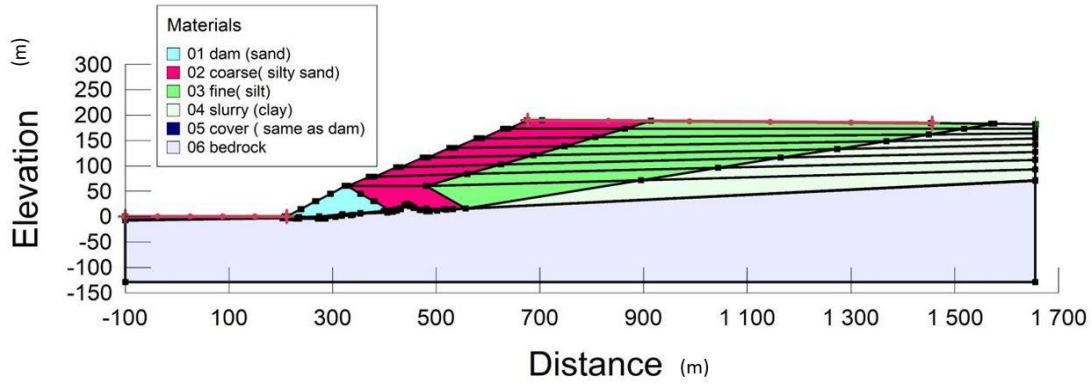

Figure 11. Initial conditions for slip surface calculations. The higher red line represents an area that is going to draw 'entry (start point) for the slip surfaces'. The lower red line represents an area that's going to draw 'exit (end point) for the slip surfaces'. The Areas between slope, start and end point are the slip surfaces. Two examples of calculation results are presented in Figure 3.

The next part of the study was to combine a seepage and stability test to see how they impact the safety of the tailing reservoir. The first step was to calculate seepage of the tailings reservoir at the time that the tailings reservoir had just been constructed. The second step was to simulate the deformation based on the results from 'seepage'. All sections were regarded as one layer instead of eight layers. Finally, this information was used to calculate the safety factor (section 2.4.1).

The boundary condition for seepage was extended to simulate when extra water is added to the model. This means that the tailings reservoir gets more water, for example, after a heavy rain. Due to the highest point is 190m, total head was set to 190 m instead of 184 m. At the left edge in Figure 12, the groundwater table still exists and total head was set to -20 m.

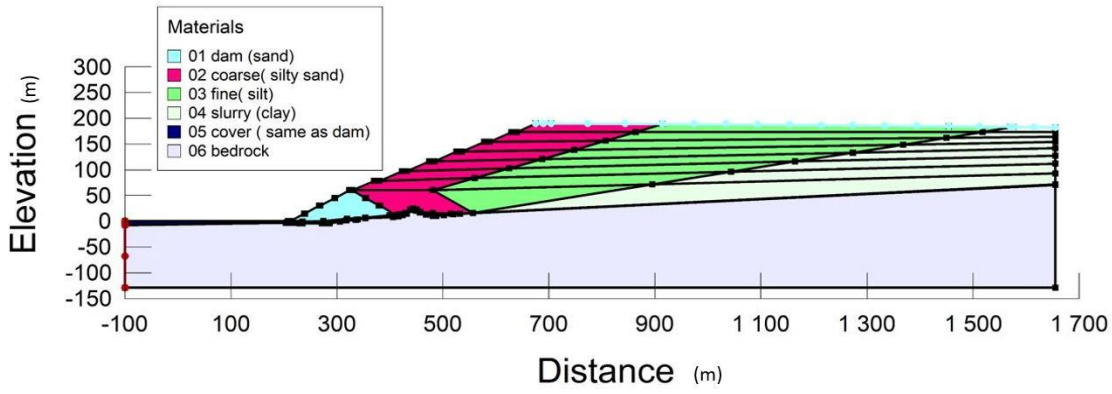

Figure 12. Boundary conditions for seepage in GeoStudio Slope/W.

4 Results

Results from the tailings reservoir model that were constructed using Seep/W, Ctran/W, Sigma/W and Slope/W are presented.

4.1 Seepage results

Using the settings in section 3.3.1 ‘Method GeoStudio Seep/W’, total head and pore water pressure were calculated and shown in Figures 13, 14, 15 and16. The blue dashed line showed where water pressure was equal to zero, i.e., it showed the groundwater level.

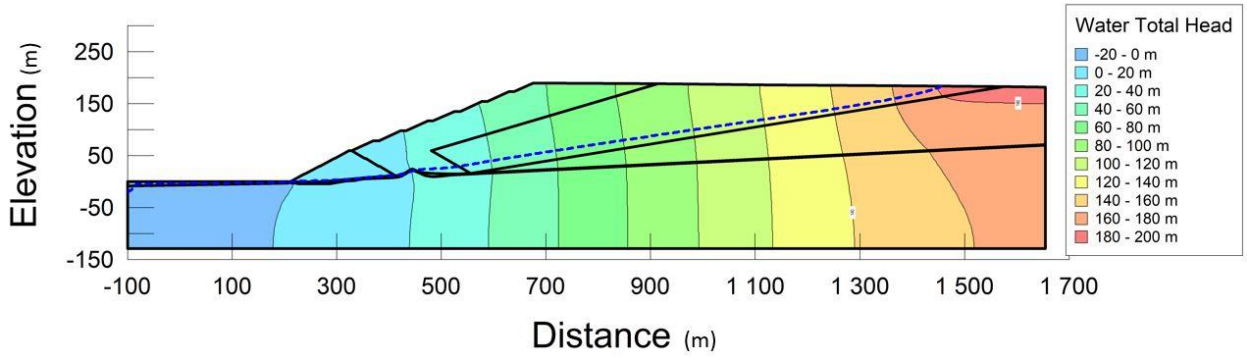

Figure 13. Total head for the tailing reservoir, steady state.

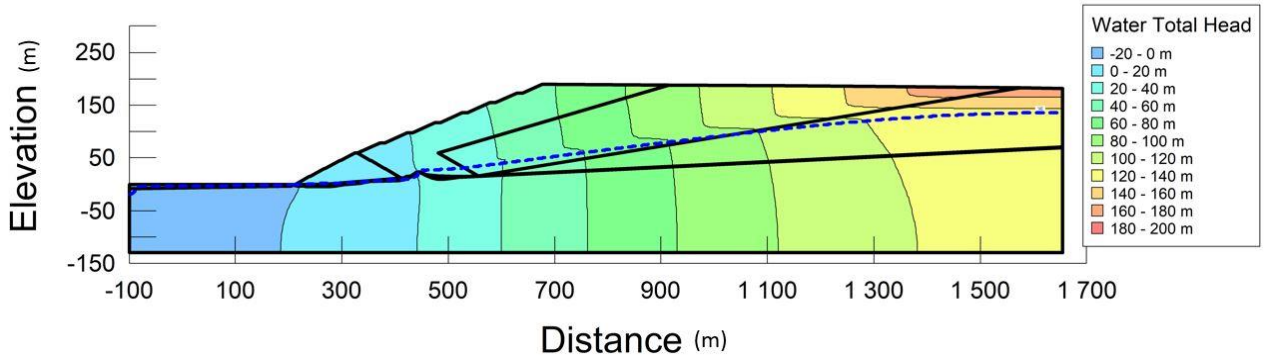

Figure 14. Total head for the tailing reservoir, after 100 years.

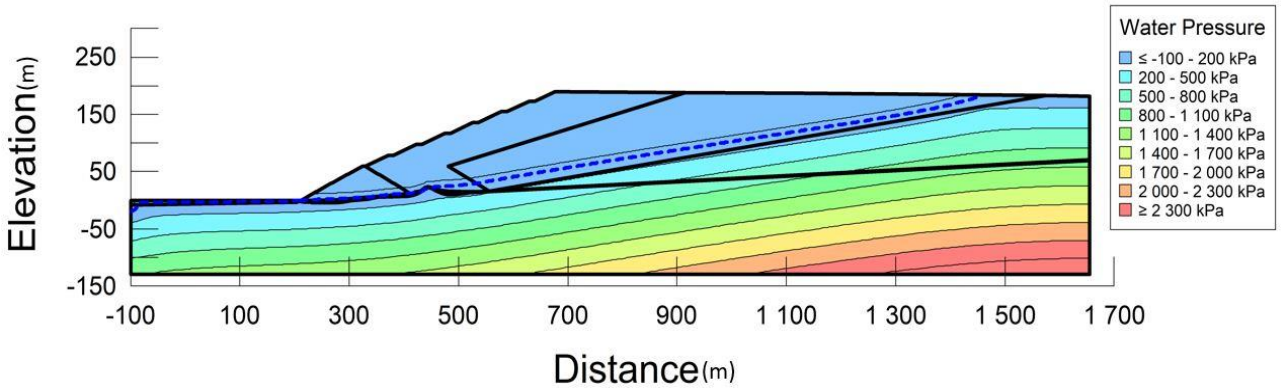

Figure 15. Pore water pressure for the tailing reservoir, steady state.

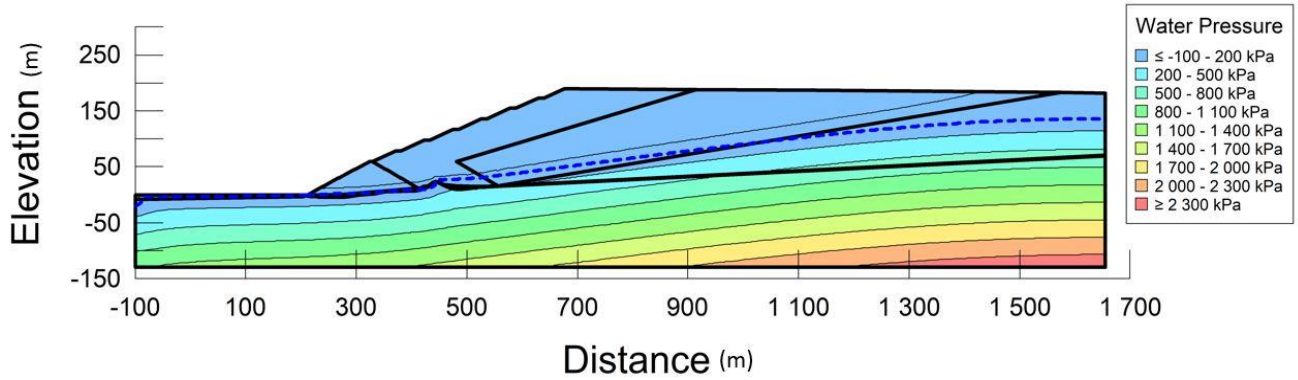

Figure 16. Pore water pressure for the tailing reservoir, after 100 years.

4.2 Contaminant transport results

The general contaminant transport is presented in the first part and the transfer of ten selected contaminant particles in the tailing reservoir is presented in the second part.

4.2.1 General movement of contaminants

Contaminant transport in the tailing reservoir during a period of 100 years is presented in Figure 17 and 18. The black arrows in figure 18 represent water flux. The white dashed line presented the isoline of contaminants with a concentration of 0.01 g/m^3, which was selected as a thousandth of the original content (10 g/m^3) in the model.

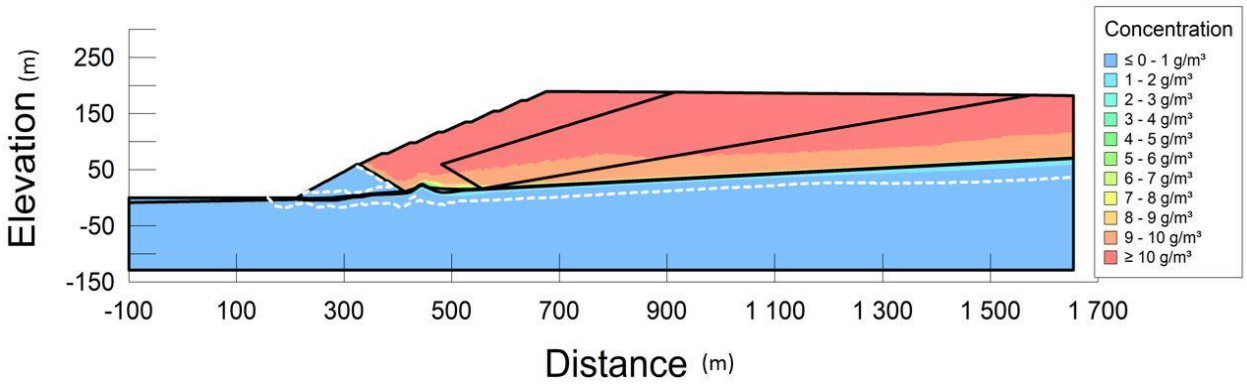

Figure 17. Distribution of contaminant concentration after 10 years. Rainwater infiltration not considered in simulation. White dashed isolines show where the contaminant concentration is 0.01 g/m^3 after 10 years.

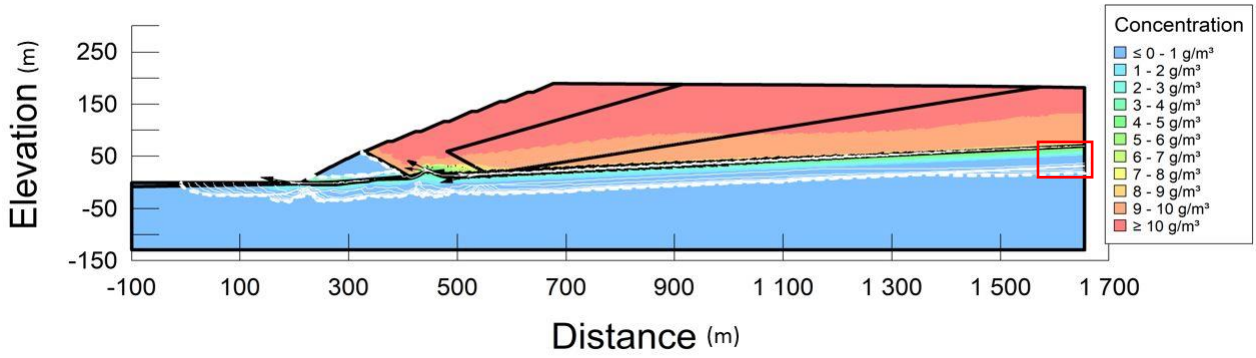

Figure 18. Distribution of contaminant concentration after 100 years. Rainwater infiltration not considered in simulation. White dashed isolines show where the contaminant concentration is 0.01 g/m^3 over a 100-year period with 10 -year intervals. The red rectangle at right is enlarged Figure 19 for details.

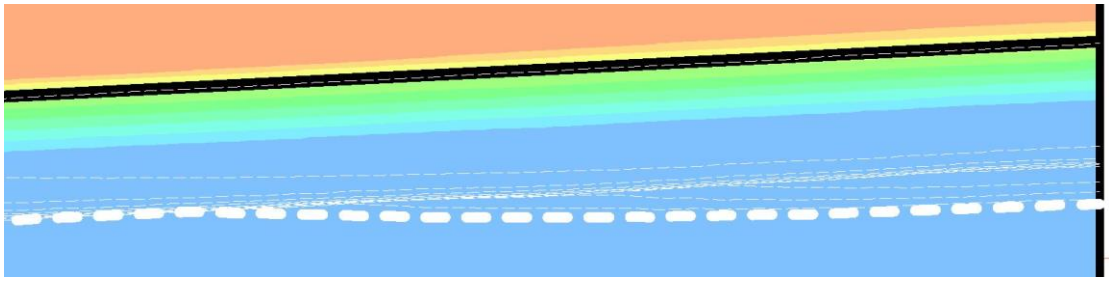

Figure 19. Enlarged region from Figure 18 to show changes in 0.01 g/m^3 concentration at 10-year intervals.

4.2.2 Particle movement

The results of the particle migration simulations are shown here. As shown in Figures 20 - 22, particle 9 moved with the highest speed and the longest distance. Particles 5, 6, 7 and 8 had

no movement, due to their locations are always above the groundwater level (see Figure 14).

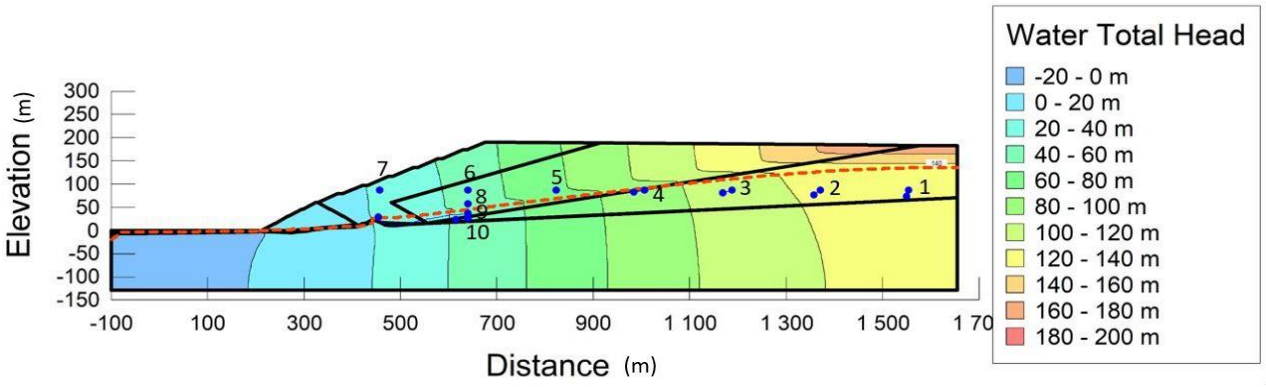

Figure 20. Displacement of ten particles in the tailing reservoir after 100 years. Blue dots represent contaminant particles and the background color shows concentration. A detailed view of particle movement is shown in Figure 22. The background color shows the total head. The red dashed line is groundwater level.

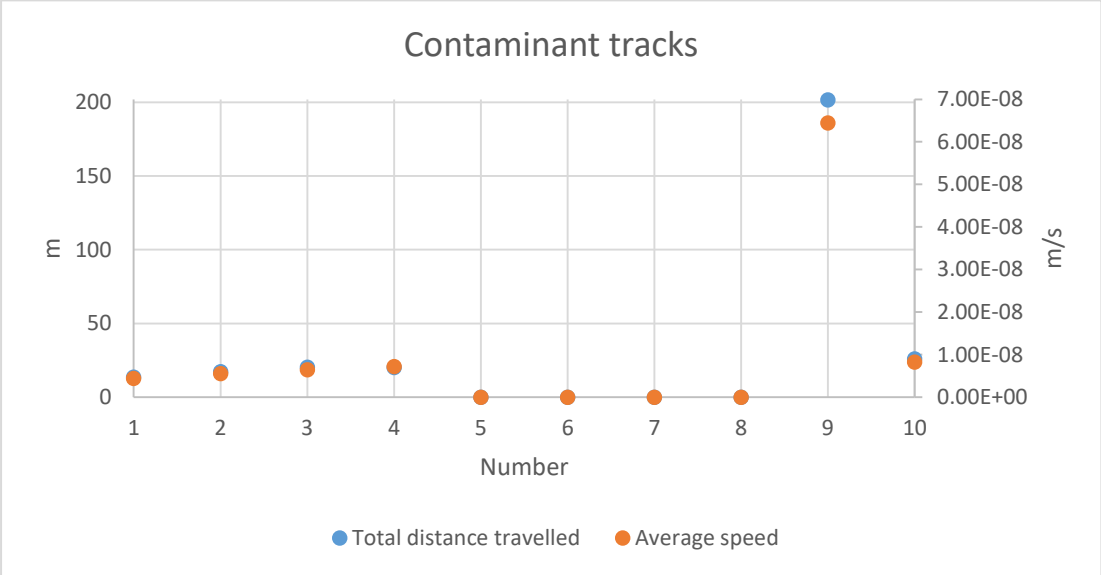

Figure 21. Distance and average speed that particles have traveled in the tailing reservoir.

According to Figures 21 and 22, particle 9 moved the furthest compared to the others. The particle traveled into the 'cover' layer which has a much higher hydraulic conductivity, dispersion and advection than the surrounding layers. This shows that adding a 'cover' layer is a useful method to drain off water and contaminants. The rest of the particles have similar velocities. Particle 1 transfers downward more than particles 2 and 3 which follow the changing of the total head.

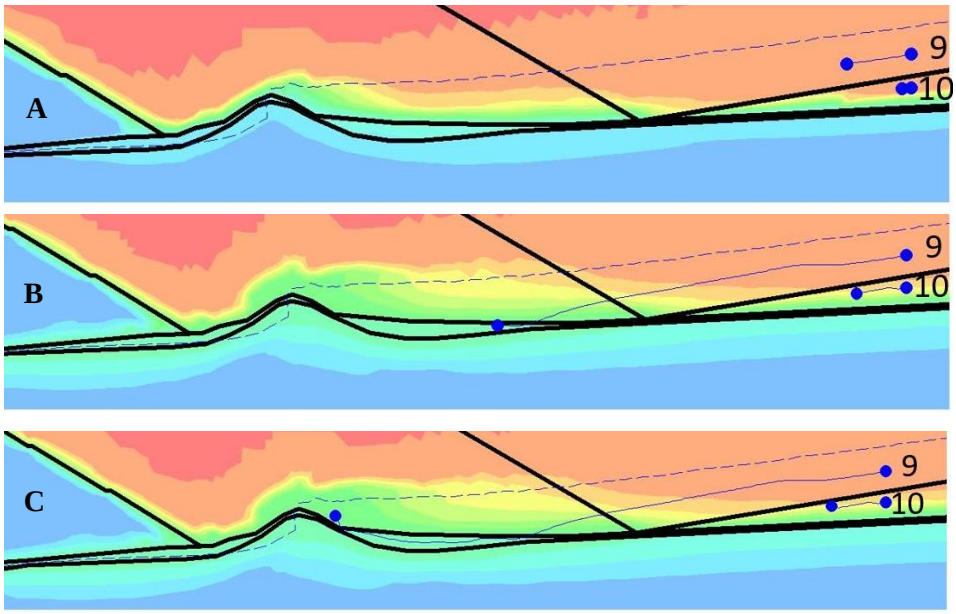

Figure 22. Zoomed in image of two particles when A) 10 years had passed, B) 60 years had passed, and C) 70 years had passed. Particle 9 and particle 10 were placed in two different sections. Particle 10 that was placed in the 'slurry' section was transported slower than particle 9 in the 'fine' section. During the first 10 years, particle 9 traveled 19.45m and particle 10 traveled 2.67m. During first 60 years, particle 9 traveled 132.73m while particle 10 traveled 1378m. Particle 9 migrated out of the 'cover' section and traveled 189.18m after 70 years, which means it traveled 56.45m during the last ten years.

4.3 Compaction

The compaction of the tailing reservoir is presented in this section. The result considered the effects of compaction during construction, so that the simulations illustrate deformation step by step, layer by layer. Figure 25 shows displacement based on layered construction, which can provide more information than strain.

In Figure 26, the color changes indicate that the greatest change in compaction occurs mostly near the slope. Near the slope, at zone 1, 2, 3 and 4, vertical displacement increases 0.5 meter for every 10 to 30 meters from the slope but in zones 5, 6 and 7, vertical displacement changes less over the same distance.

Figures 27 and 28 show the distribution from the strain. As shown in Figure 28, strains on the bedrock were low in every time series, 0 sec, 20 days, 120 days etc. The first layer next to the 'bedrock section' is the section that gained the biggest strain, and when elevation increased, the strain decreased. As time goes by and more layers are constructed, the strains on previous constructed layers increase.

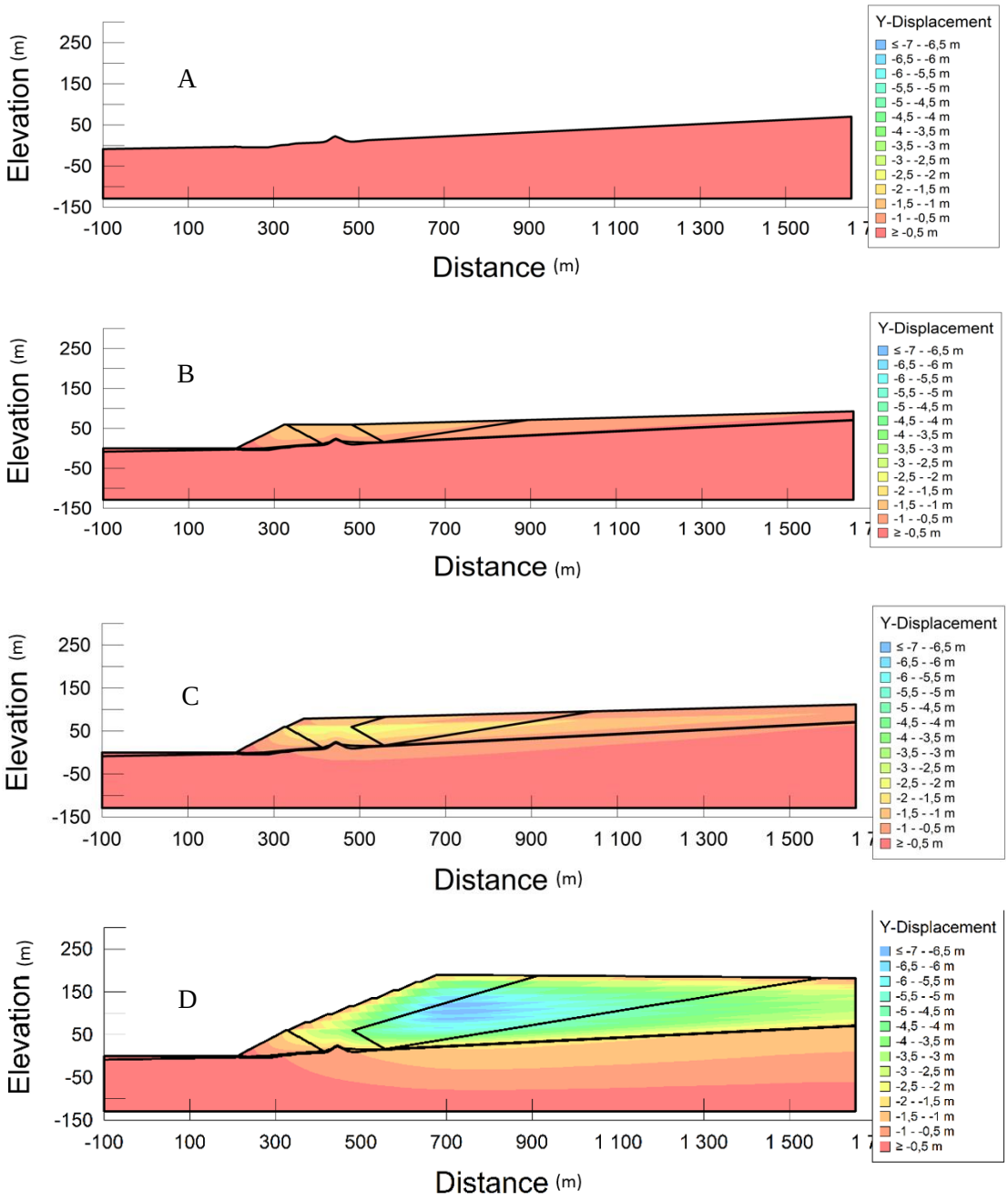

Figure 25. Compaction of tailings during deposition. A) Simulated situation on the day that construction began. There were no tailings deposited on the bedrock yet, therefore only bedrock was shown in the figure, and no displacement. B) Simulated situation at day 100, one layer tailing was deposited on the bedrock. The biggest displacement in this layer was -1.49m. Negative number in Y- direction means compaction. C) Compaction after 200 days. The biggest displacement is -2.40m. D) Compaction after 800 days, with eight layers on bedrock. The biggest displacement was -7.07m.

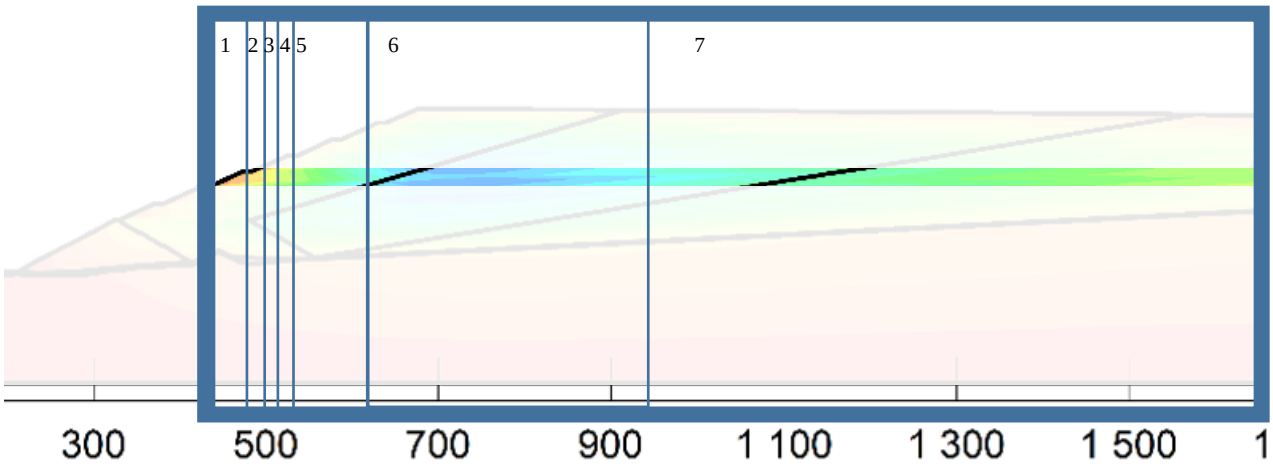

Figure 26. One of the layers from figure 25D and adds several lines to show how vertical displacement changes with color distributions.

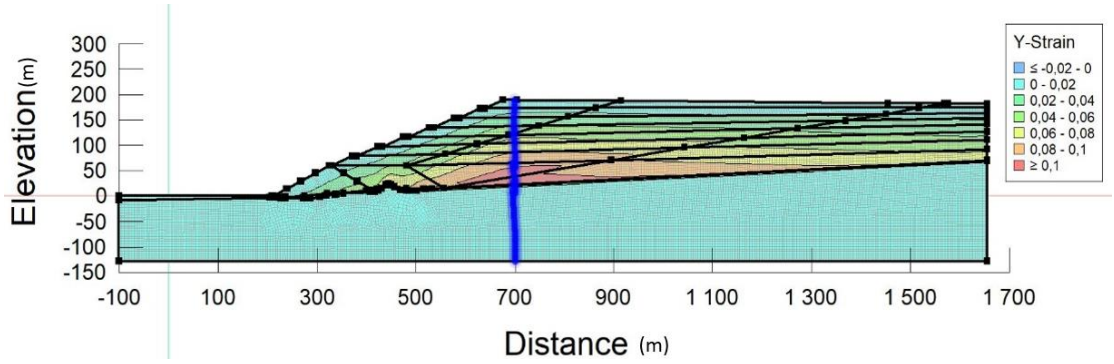

Figure 27. Shows strain in vertical direction. The blue line was a selected area. In the next figure more information about this area is presented (see Figure 28).

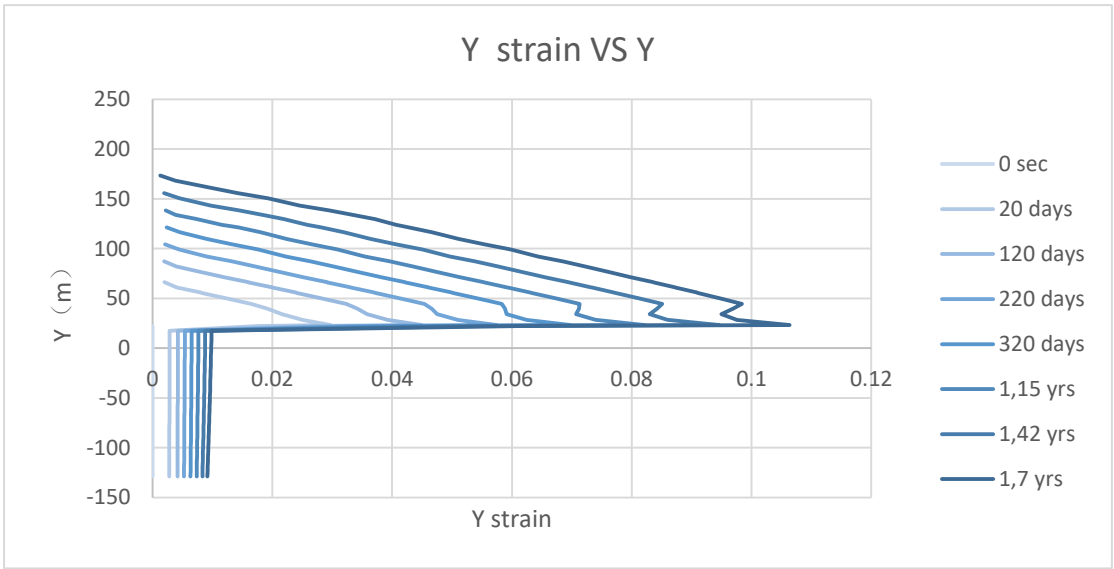

Figure 28. Strain data from selected area in Figure 27. It shows the vertical (Y) strain at

different heights during 2 years of construction time. Each line represents strain on the first day of construction of each layer.

4.4 Stability

According to the calculations from deformation without considering seepage, there are 331 slip surfaces. Five slip surfaces are depicted in Figure 29.

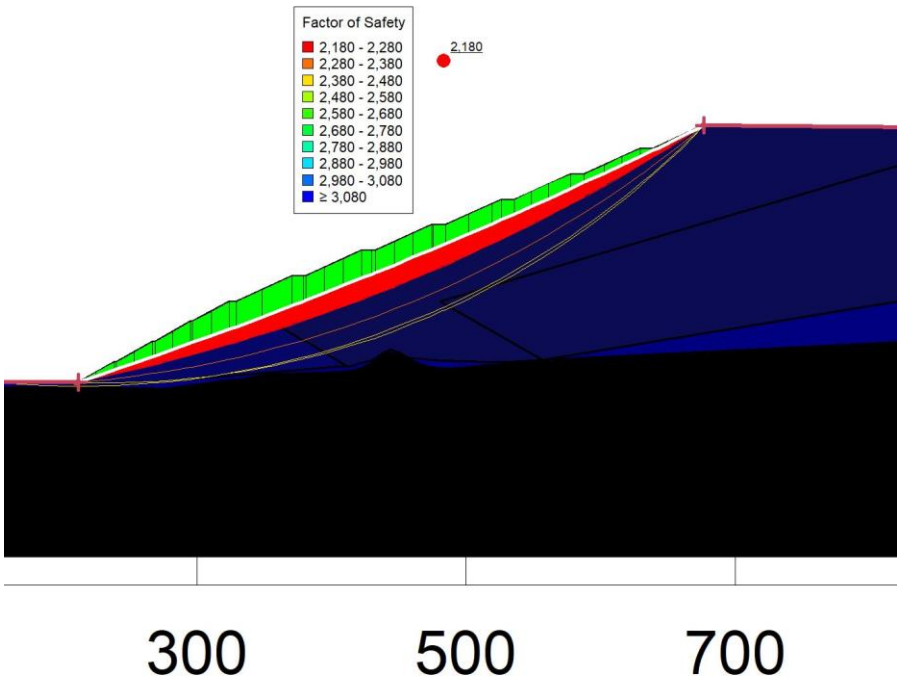

Figure 29. The five slip surfaces with lowest 'F_s' are shown. The respective 'F_s' are 2.180, 2.257, 2.329, 2.388, and 2.453 that shows with different color arc lines. The most unstable slip surface is filled with green color. The red area under the green zone is the safety zone. No water flowed out of the dam for these simulations.

In Figure 30 and 30, seepage and deformation were combined in order to do a stability test. When total head on the top surface was set to 184 m (Figure 30), the dam was still safe since the lowest 'F_s' was still greater than 1. Here, the slip surface is similar to the slip surface in Figure 29. According to Figure 31, water is seeping from the toe of the dam wall.

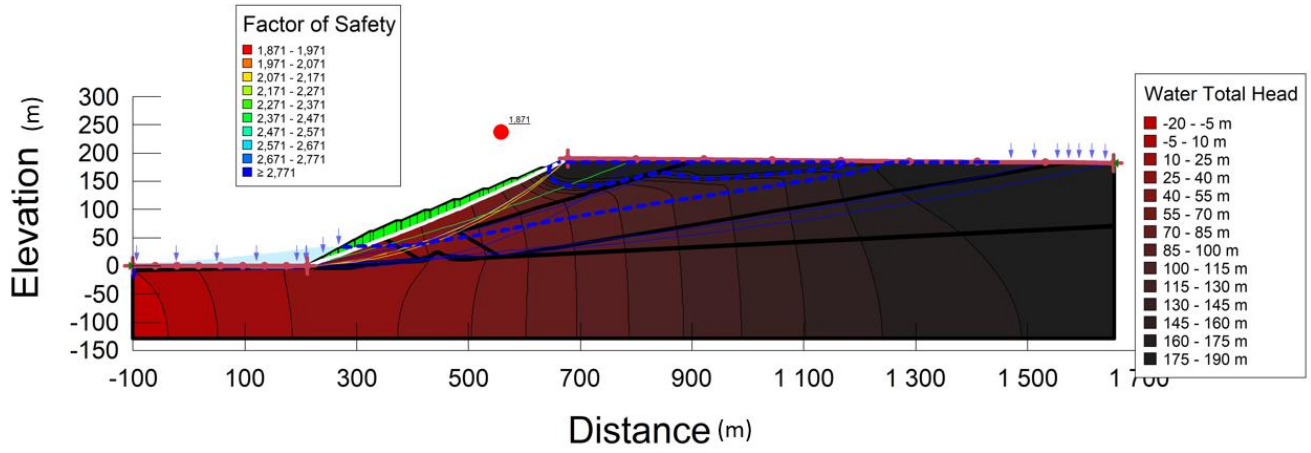

Figure 30. Slope safety based on the seepage and deformation. Total head on the top surface was 184 m. The dark blue dashed line is the groundwater level. The light blue area is water. The light blue arrows represent the water flow directions.

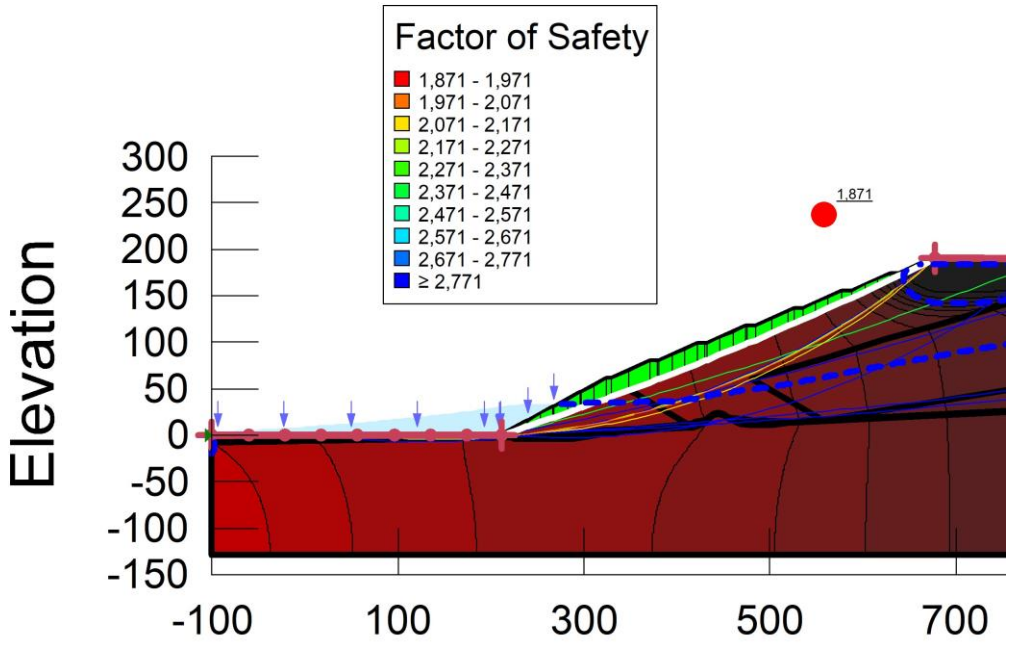

Figure 31. This figure zoomed in left part of Figure 30. Water flowed out of the dam.

In order to investigate the effect of higher pore water pressures in the reservoir, the total head in the reservoir with increased at the upper surface, as shown in Figure 32 and 32.

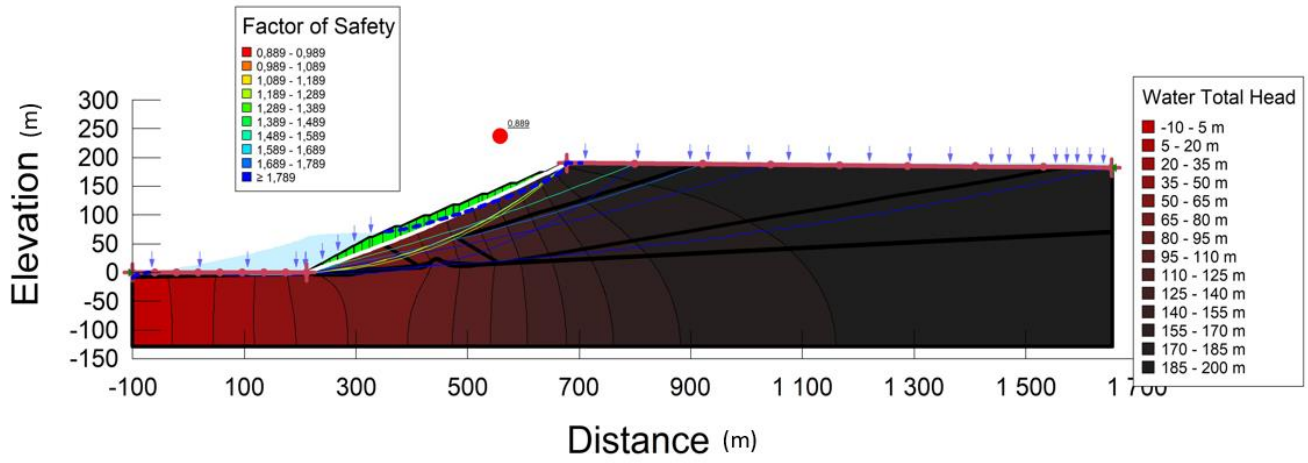

Figure 32. Slope safety based on the seepage and deformation. Total head boundary condition on the top surface was set to 190 m and groundwater at the left edge was set to -10 m.

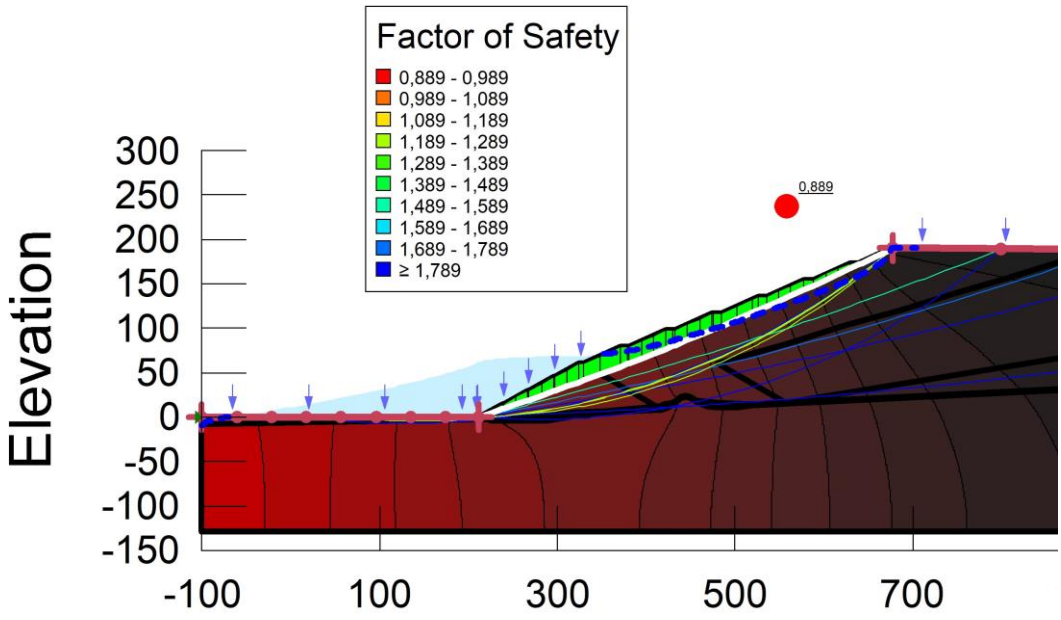

Figure 33. Enlarged region from Figure 32.

Using the boundary conditions shown in Figures 31 and 32, the lowest F_s became 0.889, which is lower than one, which means that the slope became unstable, and shear failure occurred. Water comes out from the dam, which is an unusual situation. To avoid this, a sensitivity analysis was conducted to determine which boundary condition would yield $F_s > 1$ (see Figure 34). The result of simulations are shown in Figure 34 and indicated that the safety factor F_s was highest when the total head was -20 m. It decreased when total head became lower or higher. To avoid shear failure it is worth considering optimizing the water level in front of a dam.

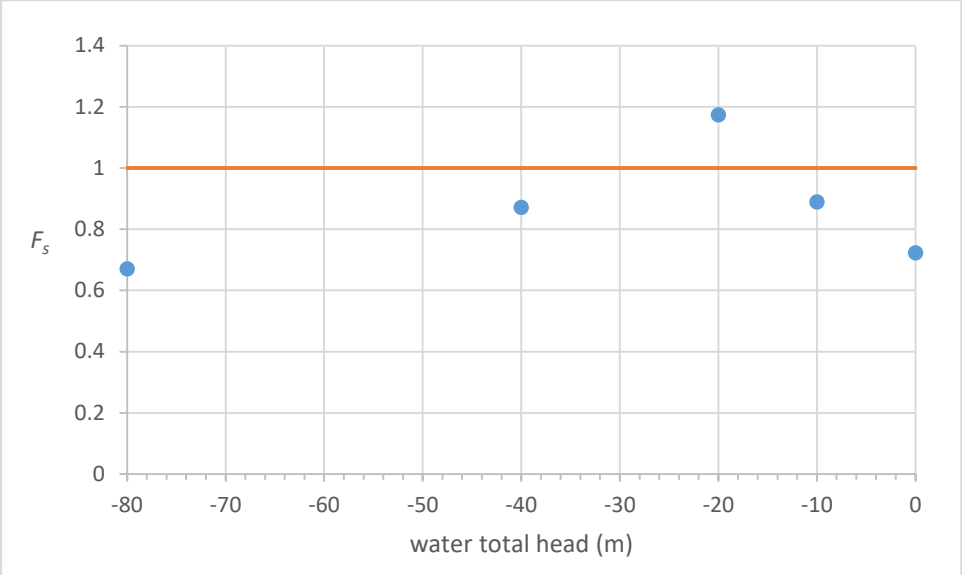

Figure 34. Safety factor as a function of variations in the total head boundary condition located to the left of the tailing reservoir. The total head boundary condition at the top surface was always 190 m.

5 Discussion

The calculation of total head in the model agrees with the expected results, indicating that the presupposed initial and boundary conditions in 'Method' were acceptable. In Figures 13 and14, the total head was highest at the upper right boundary condition and lowest at the lower left boundary condition of -20 m. In Figures 15 and 16, water pressure increased as the elevation decreased, as expected, and negative pore water pressures coincided with the unsaturated zone in the tailings. For the 100 year simulation (Figure 14), equipotential lines in the unsaturated zone are shifted to lower elevations at the boundary between the 'slurry' and the 'fine' sections, which reflects that contrast between the hydraulic conductivity of 'slurry' was lower than the 'fine' section. As water flows from higher to lower total heads, Figure 14 shows that water flow is vertical at the upper right boundary and at the water table, but otherwise flowing from right to left.

The contaminant transport simulations indicate that the contaminant in the initial dam had been slightly flushed from the dam after 100 years (Figure 18). The simulations show that much of the contaminant transport occurs in the high conductivity cover (Figure 35) that lies between the tailings and bedrock (see Table 1, Figure 6), with much of the water and contaminants coming from 'fine' and 'slurry' sections.

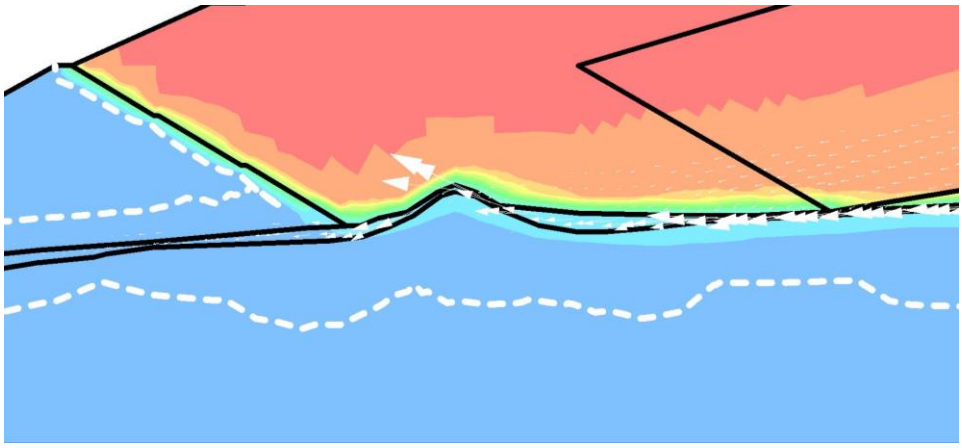

Figure 35. Zoomed in image of the contaminants transfer around the initial dam. The white arrows showed how fast contaminants moved in the tailing reservoir. The directions of the contaminant (white arrows) come from right to left in the figure.

The compaction simulations indicate, as expected, that the displacement of the tailing reservoir increased as more layers were placed on it (Figure 25A-D). The pressure created by self-weight is less at the top two layers and on the slope. By comparison, material in the middle had the highest displacement. This may depend on the layered construction. 'Bedrock' had the highest E-modulus at the beginning and E-modulus became higher when effective stress increased, therefore it could not settle as easily as other materials, which is expected for bedrock.

The model predicted that the most unsafe slip surface was quite narrow and located at the dam slope, where was the most change in displacement over the shortest distance (Figure 25D). The deformation made the slope less safe and increased the risk for shear failure. This conclusion is the same as the data provided in Yang et al. (2008), which shows that the most common reason for tailing reservoir collapse is dam slope instability.

In the slope failure and safety factor calculations, the left boundary condition was change to -10m. Although a change a of 10 m total head may not be realistic to achieve in a short time, the purpose of the stability tests was to study how water impacted the safety of the tailing reservoir in extreme cases. As shown in Figures 29 to 34 the total head played an important role in slope stability and F_s. When the total head in front of the tailing reservoir changed, the saftey factor also changed, and in this case -20 m was the most stable boundary condition since it had a safety factor higher than 1. This phenomenon can be explained by the water level increasing when total head became higher than -20 m, which decreased the friction between the slip surface and its contact surface. This in turn increased the shear force, and decreased the stability. When total head became lower than -20 m at the boundary, the difference in total head from right to left increased, which increased seepage velocity, and lowered the stability.

To compare with the previous study (Bäckström and Ljungblad, 2016), both studies showed similar distribution of the total head and water pressure in the tailings reservoir. The most

unstable part in the tailings reservoir was the slope, and the safety factors of the slope were quite high for both studies. Additionally, this work simulated the step-by-step deformation of the reservoir, and tried to explain why the slope is the most fragile part based on the contribution from deformation, but it may not be the only explanation. For future simulations, I would investigate the reason behind the phenomenon, and hope this work can be a help. I wish this work may contribute to decrease the accidents of shear failure and better understanding of contaminant transport in tailings reservoirs.

6 Conclusion

Results of the simulations have some similarity to the previous studies and indicate that the selected parameters were reasonable. Furthermore, this study found that contaminant transport is mostly related to the total head under the groundwater table. A ‘cover’ layer above a bedrock surface can accelerate the transportation of contaminants, as shown in this case. Displacement is greatest in the middle of the tailings reservoir. Strain is largest at the first layer over the bedrock. The biggest change of displacement with distance is located near the slope, and it is also where the most unstable part of dam is located. Last but not least the safety of the dam may decrease if the total head outside the reservoir dam increases.

References

Verruijt, A. (2001) *Soil mechanics*. Ames: Delft University of Technology press.

Bear, J. (1972) *Dynamics of fluid in porous media.* American Elsevier Press.

Bochove, D. Lombrana, L, M. Stringer, D.(2019). *Brazil's Deadly Dam Collapse Could Force the Mining Industry to Change.* Bloomberg Businessweek, 07 october Available from: https://www.bloomberg.com/news/articles/2019-02-20/brazil-s-deadly-dam-collapse-could-force-the-mining-industry-to-change [2019-10 -07]

Bäckström, J. and Ljungblad, M. (2016) *Safety Evaluation of the Zhaoli dam*. Master thesis, Civil Engineering Program in Energy Systems, Uppsala University ISSN:1650- 8300, UPTEC ES 16031.

Clancy, L.J. (1975) *Aerodynamics*. Wiley.

Comsol (2017) *The Finite Element Method (FEM).* Comsol. Available from: https://www.comsol.com/multiphysics/finite-element-method [2019-10-07]

Davies, M. P. and Martin, T. E. (2000). *Upstream constructed tailings dams - A review of the basics.* A.A. Balkema.

Domenico, P.A and Schwartz, W. (1998) Physical and Chemical Hydrogeology. 2nd Edition. John Wiley & Sons Inc., New York.

Blowes, D, W. Weisener, G. (2003) *Treatise on Geochemistry.* ScienceDirect®. Available from: https://www.sciencedirect.com/topics/agricultural-and-biological-sciences/mine-tailings [2020-04-08]

GEOSLOPE International Ltd (2012) *Contaminant modeling with CTRAN/W.* [Brochure]. Calgary, Alberta, Canada.

GEOSLOPE International Ltd (2012) *Seepage Modeling with SEEP/W*. [Brochure]. Calgary, Alberta, Canada. Available from: http://downloads.geo-slope.com/geostudioresources/8/0/6/books/seep%20modeling.pdf?v=8.0.7.6129 [2019-10-07]

GEOSLOPE International Ltd (2013) *Stress- Deformation Modeling with SIGMA/W.* [Brochure]. Calgary, Alberta, Canada.

GEOSLOPE International Ltd (2015) *Stability Modeling with Slope/W*. [Brochure]. Calgary, Alberta, Canada.

GEOSLOPE International Ltd (2018) *Heat and mass transfor modeling with GeoStudio*. [Brochure]. Calgary, Alberta, Canada.. Available from: http://downloads.geo-slope.com/geostudioresources/books/9/0/Heat%20and%20Mass%20Transfer%20Modeling-20180125.pdf [2019-10-07]

Hu, L. Professor at the department of hydraulic engineering. Commented, 2019

Li, G. Zhang, B & Yu, Y. (2013) *Soil mechanics. 2.* Edition. Ames: Tsinghua University press.

Craig, R, F. (2004). *Craig's Soil Mechanics*. Taylor and Francis Group.

SGU (2020). *Lecture 4: Mining Waste.* Geological survey of Sweden. Available from: https://www.sgu.se/en/geointro/lecture-4-mining-waste/[2020-04-08]

Song, S. Yan, S. Liu, X. (2017). *Influence of iron ore tailings powder on the performance of high fluidity concrete.*cnki. Available from: http://en.cnki.com.cn/Article_en/CJFDTotal-HLTF201711018.htm [2019-10-07]

Vick, S.G. (1983). *Planning, design, and analysis of tailings dams.* New York: John Wiley & Sons Inc.

Wang, H. (2008) *Dynamics of Fluid flow and contaminant transport in porous media.* Higher Education Press.

Wong, M. H. Tam F.Y (1977) *Soil and vegetation contamination by iron- ore tailings.* Elsevier Ltd.

Yang, L. Li, Q. Cheng, W. Wang, Y. (2008). The analysis of main risk factors about tailings dam accidents at home and abroad. CNKI. Available from: http://en.cnki.com.cn/Article_en/CJFDTOTAL-LDBK200805009.htm [2019-10-07]

Appendix

Nomenclature

Greek

Denomination	Symbol	Unit
Angle	ϕ	-
Decay constant	λ	s^{-1}
Effective stress	σ'	Pa
Isothermal compressibility of water	β_w	$4.8x10^{-10}$ kPa^{-1} at 10 ºC
Mass density of water	ρ_w	kg/ m^3
Matric suction	φ	Pa
Normal stress	σ_n	Pa
Normal stress acting on x-plane	σ_x	-
Normal stress acting on y-plane	σ_y	-
Normal stress acting on z-plane	σ_z	-
Poisson's ratio	υ	-
Shear Stress	τ	Pa
Shear stress on xy- plan	τ_{xy}	Pa
soil dry bulk density	ρ_d	kg/ m^3
Soil structure compressibility	β	Pa^{-1}
Specific weight	γ_w	N/m^3
Strain and strain on different directions	$\Delta\varepsilon, \varepsilon_x, \varepsilon_y, \varepsilon_z$ τ	-
Tortuosity factor		-
Total stress	σ	Pa
Unit weight on xy- plan	γ_{xy}	N/m^3
Volumetric content, air content	θ_a	m^3/m^3
Volumetric content, water content	θ_w	m^3/m^3

Latin

Denomination	Symbol	Unit
Acceleration due to gravity	g	m/s^2
Area filled with water	A_w	m^2
Coefficient of diffusion or dispersion, diffusion of water vapor in soil	D_v	m^2/s
Cohesion	c	-
Compressibility coefficient	a	-
Diffusion	D^*	m^2/s
Diffusivity of water vapor in air at given temperatur	D_{vap}	m^2/s
Elastic modulus	E	Pa
Elevation	z	m
Flow velocity	v	m/s
Flow speed in x direction	v_x	m/s
Flow speed in z direction	v_z	m/s
Fluid pressure	u	Pa
Friction moment	M_R	Nm
Gas constant	R	8.314472 J/K/mol
Hydraulic conductivity coefficient	$k, k_x, k_{xz} k_{zx}$	m/s
Hydraulic conductivity of isothermal liquid water	K_w	m/s
Hydraulic gradient	i_x, i_z	m/m
Hydraulic head	h	m
Hydrodynamic dispersion	D	m^2/s
Initial dispersity	D_0	m^2/s
Longitudinal dispersivity coefficient	α_L	-
Longitudinal mechanical dispersion coefficient	D'_L	m^2/s
Mass concentration	C	kg/ m^3
Mass rate of change due to flow	$\dot{m}_{st}$	kg/s
Mass rate of change due to flow of liquid water	$\dot{m}_w$	kg/s
Mass rate of change due to flow of water vapor	$\dot{m}_v$	kg/s

Denomination	Symbol	Unit
Mass rate of change due to flow, flow out of a control volume	$\dot{m}_{out}$	kg/s
Mass sorbed per mass of solids	S^*	kg/m^3
Mechanical dispersion	D'	m^2/s
Molar mass	M	kg/mol
Oedometric modulus	E_s	Pa
porosity	e	-
Pressure of pore water	u_w	Pa
Safety factor	F_s	-
Seepage velocity	u_d	m^2/s
Slide moment	M_s	Nm
Slope of the volumetric water content function	m_w	m^2/N
Soil skeleton area	A_s	m^2
Source flow	Q	s^{-1}
Stored mass rate of change of all water stored in REV (representative elementary volume)	$\dot{M}_{st}$	kg/s
Stored mass rate of change of dissolved mass phase in REV	$\dot{M}_{dp}$	kg/s
Stored mass rate of change of liquid water stored in REV	$\dot{M}_w$	kg/s
Stored mass rate of change of mass added to REV	$\dot{M}_S$	kg/s
Stored mass rate of change of of adsorbed mass phase in REV	$\dot{M}_{ap}$	kg/s
Stored mass rate of change of water vapor stored in REV	$\dot{M}_v$	kg/s
Temperature	T	K
The total head	H	m
Total area	A	m^2
Total vertical stress on a surface	$\sum_{i=1}^{n} P_{svi}$	m^2 Pa
Transverse dispersivity coefficient	α_T	-
Transverse mechanical dispersion coefficient	D_T'	m^2/s
uniaxial stress	Δp	Pa
Vapor pressure	p_v	Pa
Volume of air	V_a	m^3

Denomination	Symbol	Unit
Volumetric coefficient of thermal expansion at constant pressure	α_w	K^{-1}
Volumetric flow rate	q	m^3/s
Volumetric flux of liquid water	q_w	$m^3/s/m^2$